Overexpression of DnaJ chaperones in ameliorating toxicities associated with FUS and TDP-43

Snehal Ahire[1], Tania Bose[1, #]

1: Dept. of Biotechnology, with jointly merged Institute of Bioinformatics and Biotechnology (IBB), Savitribai Phule Pune University, Ganeshkhind, Pune 411007, India

#: corresponding author (ORCID 0000-0002-5478-0407)

Email: tania.bose@gmail.com; tbose@unipune.ac.in (Tania Bose, corresponding author)

Graphical abstract

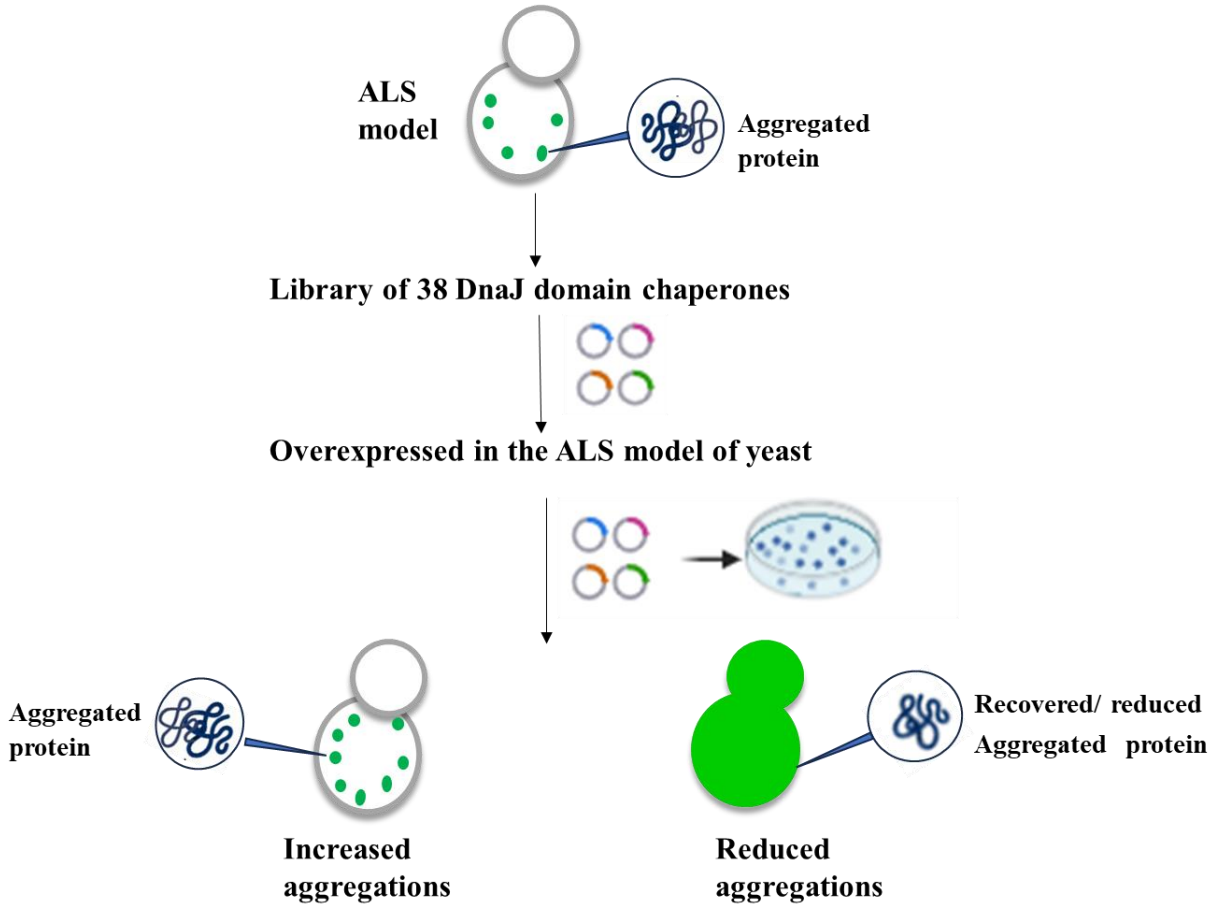

Abstract

Amyotrophic Lateral Sclerosis (ALS) is an adult-onset neurodegenerative disease. It primarily affects the motor neurons, leading to muscle weakness and eventually death of the patients. Various factors, such as genetics, environment, age, etc, are involved in the etiopathogenesis of ALS. As ALS is a highly challenging and complex disease involving various pathogeneses linked with progressive motor neuron degeneration, it is difficult to have a single therapeutic target against this disease. ALS mutants of TDP-43 and FUS are showing slow growth as well as protein aggregation in the cytoplasm in yeast. Our study involves cloning of 38 *Drosophila* DnaJ domain chaperones and overexpressing them in a yeast ALS model. After the interaction of mutants TDP-43 and FUS with the DnaJ domain chaperones, they were categorized into suppressors and enhancers. The major hits on our screen were CG7872, Hsc70-4, and Mrj, which rescued TDP-43 toxicity by reducing protein aggregation and slow growth in yeast cells. In FUS, slow growth and protein aggregation are reduced with the chaperones CG32641 and CG6693, resulting in a lowering of FUS toxicity. On the other hand, chaperones CG2911, CG2790, and CG8476 in presence of TDP-43 overexpression, grows slower with an increase in the number of aggregates in yeast cells. These chaperones increase the toxicity of TDP-43. Similarly, in FUS, Hsc20, CG7130, CG2911, and JdpC also showed slow growth phenotype and an increase in protein aggregation in yeast cells. These chaperones enhance the toxicity of FUS.

This screening will enhance our understanding of the ALS pathology, and the chaperones identified in this study can serve as neuroprotective agents for ALS.

Keywords: neurodegenerative disease, TDP-43, FUS, yeast, ALS, DnaJ domain chaperones, Hsp40, ALS, RNA binding proteins

Abbreviations

ALS Amyotrophic Lateral Sclerosis

TDP-43 TAR DNA binding protein 43

FUS Fused in Sarcoma

HSPs Heat shock proteins

GFP Green fluorescent protein

1.0 Introduction

ALS involves an interplay of different epigenetic genes associated with its pathogenesis. These genes include SOD1, FUS, TARDBP (TDP-43), VAPB, VCP, and OPTN (Cirulli et al., 2015; Ghasemi & Brown, 2018; J. O. Johnson et al., 2010; Rosen et al., 1993). These genes are found in all types of pathophysiology associated with ALS. ALS is found in two forms: sporadic and familial. ALS also results from family history and lifestyle factors, including smoking and dietary factors (Armon., et al 2009; Jong et al., 2012).

From our study, we focus on the cellular toxicity and protein aggregation phenotypes of ALS (B. S. Johnson et al., 2008a). In this study, two ALS mutants, TDP-43 and FUS, when transformed with 38 DnaJ domain chaperones, show either slow or enhanced growth combined with minimal or increased in protein aggregation, respectively.

Studies from other reports reveal the presence of pathogenic protein aggregates in mutant SOD-1 ALS cases (Watanabe et al., 2001). Protein aggregation is due to the failure of protein quality control system (PQC) failure to handle folding and the failure of degradation of misfolded proteins. (Mogk & Bukau, 2006). Protein aggregation is not always toxic. Sometimes, protein aggregation can be a protective storage mechanism. However, within the cell, depending on

the location and size of protein aggregates, these may be considered toxic (Kampinga et al., 2016)

Neurodegenerative diseases like ALS, Alzheimer's, Huntington's, and Parkinson's have a protein aggregation trait, a specific protein that can fold into an alternative stable form, leading to protein aggregation and accumulation as fibrillar deposits in tissues (Carrell & Lomas, 1997; Goedert, 2004; Martindale et al., 1998).RNA processing pathways and RNA-binding proteins are involved in the etiopathogenesis of ALS (Gitler & Shorter, 2011a; Lagier-Tourenne & Cleveland, 2009). Many of the genes associated with ALS pathogenesis are RNA-binding protein (RBP) genes, including TDP-43, FUS, Ataxin-2, TAF15, EWSR1, and matrin3 (Couthouis et al., 2011; Elden et al., 2010a; Malik et al., 2018; Ticozzi et al., 2011). All these genes share structural similarities, including RNA-binding domains, and exhibit some functional similarities, as they are involved in RNA metabolism and localize in stress granules.

TDP-43 and FUS have RNA-binding domains, and after mutation, both genes have been reported to be toxic in multiple studies. In 2006, Arai and Newmann found TDP-43 to be an essential component of ubiquitinated protein aggregates in FTLD-U and sporadic ALS (Arai et al., 2006). In ALS, when TDP-43 is derived from the damaged central nervous system, toxic TDP-43 is found in hyperphosphorylated form, cleaved to obtain a C-terminal fragment, and ubiquitinated (Neumann et al., 2006a). FUS also exhibits ubiquitous expression, similar to TDP-43, and its expression is independent. After the missense mutation, FUS also forms cytoplasmic aggregates in neurons (Vance, Rogelj, Hortobágyi, et al., 2009). In 0.4% of familial ALS cases, FUS/TLS mutations were found (Kwiatkowski et al., 2009a; Vance, Rogelj, Hortobágyi, et al., 2009). Although TDP-43 and FUS have RNA-binding domains and similar cytoplasmic aggregation properties, their toxicity mechanisms have very subtle differences (Sun et al., 2011).

We used *Drosophila* DnaJ domain chaperones, i.e Hsp40, which help in protein folding. These are the proteins that help chaperones in protein folding. These -binding molecules help to fold the proteins by binding Hsp70 or Hsp90, or both. DnaJ chaperones can induce or inhibit the ATP hydrolysis activity of Hsp70 and Hsp90 chaperones(Bar-Lavan et al., 2016; Tsai & Douglas, 1996). There are different Hsp40s in mammals, many of which follow the categories based on their domain architecture (Cheetham & Caplan, 1998). Most of them are classified into two groups: J domain proteins and tetracopeptide repeats, i.e., TPR (Caplan, 2003). Together, they form a network to modulate the functions, identifies a subset of misfolded proteins which acts as a substrate and interacts with other chaperones and co-chaperones (Caplan, 2003).

There have been reports using DnaJ library in yeast to investigate protein aggregation in ALS. We further attempted this study using an overexpression screening to accompany the earlier studies to answer the aggregation and disaggregation properties of DnaJ domain chaperones. Multiple studies have shown that heat shock proteins and chaperones help to reduce the toxicity of mutant TDP-43 as well as FUS. In HEK293 cells, overexpression of HSF-1/DNAJB21/HSP70 shows reduced cytoplasmic protein aggregation caused by mutant TDP-43 (Vance, Rogelj, Hortobágyi, et al., 2009). Previous work has shown that HSP40 chaperone Sis1, plays a role in protein folding, transport of misfolded proteins, and catabolism of ubiquitin-dependent misfolded proteins. When Sis1 is overexpressed in TDP-43 cells, it lowers the toxicity of TDP-43. Its mammalian homolog, DnaJB1, when overexpressed in rodent primary cortex, also lowers TDP-43 toxicity in neurons (Park et al., 2017). In HeLa cell line, it was observed that HSP70 prevents amyloid aggregation caused by the mutant TDP-43 and prevents the liquid-to-solid transition (Gu et al., 2021).

There are very few studies that show HSPs can increases TDP-43 toxicity, one in vivo study on *C. elegance* showing that HSP 90 chaperone contributes to increase in TDP-43 toxicity (Garcia-Toscano et al., 2024).

TDP-43 and FUS both undergo liquid-to-solid phase separation (Li et al., 2018; Molliex et al., 2015). This process results in the formation of liquid-like sections in the cytoplasm during stress and at the site of DNA damage. The pHSP 40 chaperones Hdj2 (DNAJA1) and Hdj1 (DNAJB1) assist FUS in undergoing phase separation. Additionally, Hdj1 aids the phase-separated FUS in inhibiting amyloid and protein aggregation within the cell(Gu et al., 2020). The small heat shock protein Hsp27 is co-localized with FUS and prevents their phase separation by binding FUS to the low complexity region, thereby helping to avoid the formation of stress granules in the cell model (Z. Liu et al., 2020).

Chaperones are the proteins that assist in the folding or unfolding of large proteins and differentiate between misfolded proteins, unfolded proteins, and aggregated proteins with specific biological functions (Beissinger & Buchner, 1998). The main cellular function of the chaperones is assisting in the quality control of protein folding. Not all chaperones can prevent aggregation. Some chaperones assist in restoring correct folding and denatured protein function and aid in the assembly and disassembly of proteins. They also help fold *de-novo* proteins and, in the translocation and disaggregation of protein aggregates (Bar-Lavan et al., 2016). Chaperones are classified into five main families based on their molecular mass and sequence similarities (Bascos & Landry, 2019).

In prokaryotes and eukaryotes, Heat shock proteins (HSPs) are ubiquitously conserved for the survival of stressful conditions like heat stress (Morimoto & Santoro, 1998). It can cause harmful damage to cellular architecture and interfere with vital cellular functions. To combat heat stress, the cell activates its classical pathway, whereby it expresses heat shock proteins for a shorter period for cell survival and maintains protein homeostasis (Lindquist, 1981).

131 In our study, we have used the yeast model to focus on the mechanism of cellular toxicity and
132 protein aggregation phenotype in both TDP-43 and FUS (B. S. Johnson et al., 2008b, 2009;
133 Sun et al., 2011). Our observation supports enhanced and rescued protein aggregation and
134 cellular growth via interaction of DnaJ domain chaperones with ALS mutants. We found
135 potential suppressors and enhancers with the interaction of DnaJ domain chaperones. To check
136 our findings, we expressed 38 DnaJ domain chaperones from flies in yeast (Deo et al., 2024;
137 Desai et al., 2024).
138 Gitler and colleagues established yeast as a model to study ALS related to TDP-43 [(B. S.
139 Johnson et al., 2008a). The same group also reported using yeast for genome-wide screening
140 of FUS to uncover the mechanisms of the cellular pathways and the genes involved in FUS
141 toxicity (Sun et al., 2011). Taking cues from these studies, we explore the interactions between
142 TDP-43 and FUS with Drosophila DnaJ domain chaperones, including their potential
143 suppressors and enhancers.
144 This study focuses on two genes associated with ALS, namely TDP-43 and FUS. Despite
145 extensive research, there is still limited information available about its cure and precise cause.
146 In this work, we discuss screening both genes by transforming with *Drosophila* DnaJ domain
147 chaperones and identifying potential suppressors and enhancers. This will help identify the
148 possible interactors and their network with respect to the DnaJ domain chaperones.
149 Our study emphasizes protein aggregation and cellular toxicity in ALS mutants, involving the
150 overexpression of TDP-43 and FUS genes. We screened 38 DnaJ domain chaperones of
151 *Drosophila*, which include CG30156, CG5001, Mrj, DnaJ60, CG2911, CG6693, JdpC,
152 CG9828, CG4164, CG2887, CG12020, JdpA, CG10565, Tpr2, Csp, CG7394, CG7130,
153 CG8476, CG7872, Hsc20, Sec63, P58IPK, CG43322, CG7133, CG7556, CG14650, CG32641,
154 CG11035, CG10375, CG17187, DnaJ1, CG3061, CG8531 and CG7387. In addition, there are,
155 two Hsc70 (Hsc70-1, Hsc70-4) and Hsp70 (Hsp70Aa and Hsp70Bb) chaperones. We chose

156 only those chaperones that play a role in protein folding, listed in **Supplementary Table S2**.
157 Their function and activity are the same as the human homologs (Gaudet et al., 2011; R. et al.,
158 2012).
159 We found that chaperones CG7872, Mrj, and Hsc70-4 suppress the toxicity of TDP-43, and
160 chaperones CG32641 and CG6693 suppress the toxicity of FUS.
161 These chaperones are found to play a protective role in other disease conditions as well.
162 DNAJC25 is an orthologue of CG7872, localised in the cytoplasm, and plays a role in
163 hepatocarcinoma suppression (LIU et al., 2012a).
164 After mutation, Mrj is found in disease conditions like frontotemporal dementia and limb-girdle
165 muscular dystrophy type 1(Yabe et al., 2014). In some cases, in mouse and *Drosophila*, Mrj
166 inhibits Huntington PolyQ aggregation [48,36]. In addition to Huntington, Mrj also reduces the
167 α-synuclein aggregation in Parkinson's disease with co-chaperone Hsp70 (Aprile et al., 2017).
168 In both Huntington's and Parkinson's disease, Mrj suppress the toxicity of Htt and α-synuclein
169 disease-causing proteins, but no such evidence has been found in the ALS-causing gene TDP-
170 43. Also, Hsc70 is a co-chaperone of DnaJ domain chaperones and is also found to improve
171 the TDP-43 toxicity in sporadic ALS patients (Arosio et al., 2020; Richter et al., 2010). Human
172 orthologue of Hsc70-4 is HSPA8 which has been reported to be involved in clearance of
173 misfolded proteins (T. Liu et al., 2012; Stricher et al., 2013).
174 DNAJC9 is the human orthologue of CG6693 and has been found to play a role in cancer
175 (Zhang et al., 2020). Also takes part in histone chaperone function with the help of the co-
176 chaperone Hsp70 (Hammond et al., 2021). DNAJB9, is also a human orthologue of chaperone
177 CG32641 and is found associated with ER degradation machinery, and also interacts with
178 CFTR and rescues the cystic fibrosis-causing gene Δ F508 (Huang et al., 2019; Lai et al., 2012).
179 Some chaperones can enhance the toxic phenotype, specifically slow growth and protein
180 aggregation in both mutant FUS and TDP-43. We found that chaperones CG2911, CG2790,

181 and CG8476 are enhancers of TDP-43 toxicity, while chaperones Hsc20, CG2911, CG7130,
182 and JdpC enhances FUS toxicity. Previously, they were found to contribute to toxicity in certain
183 diseased conditions (D. Liu et al., 2024; Thomson & Dinger, 2016; Uhrigshardt et al., 2013;
184 Veenma et al., 2018).
185 To develop TDP-43 and FUS models in *Saccharomyces cerevisiae,* we used galactose-
186 inducible plasmids pRS426 Gal-TDP-43-GFP and pAG416 Gal-FUS-YFP, respectively.
187 Mutant TDP-43 and FUS shows slow growth and protein aggregation in yeast cells at
188 permissive temperature. When these two mutants were expressed with 38 DnaJ domain
189 chaperones, we found some chaperones suppressed the toxicity, while some chaperones
190 enhance the toxicity of the mutants, TDP-43 and FUS.
191

192 **2.0 Results**

193 **2.1 Yeast model of TDP-43 and FUS: growth assay and protein aggregation**

194 We constructed TDP-43 and FUS yeast models with TDP-43 and FUS plasmids pRS426 Gal-
195 TDP-43-GFP and pAG416 Gal-FUS-YFP, respectively [method adopted from (Deo et al.,
196 2024; Desai et al., 2024). This construct has a Ura marker with a GFP tag at the C-terminal
197 and a galactose-inducible promoter. **(Supplementary Fig S1)**

198 The TDP-43 mutant results in slow growth and protein aggregation in yeast cells, indicating
199 pathogenicity (B. S. Johnson et al., 2008a). Similarly, the FUS mutant shows slow growth and
200 protein aggregation, indicating pathogenicity in yeast cells (Sun et al., 2011).
201 We used an empty vector as a control, and TDP-43 and FUS for determining ALS toxicity
202 (Mogk, 1999; Tomoyasu et al., 2001). The spot dilution assay of TDP-43 and FUS mutants
203 shows slow growth compared to the control in Gal-Ura **(Supplementary Fig S2a).**
204 A quantitative study of both mutants was done using a 48-hour growth assay. TDP-43 and FUS
205 cultures were added in triplicates to a 96-well plate at 30°C with orbital shaking. Growth assay

206 of TDP-43 and FUS shows slowdown of TDP-43 and FUS growth in liquid medium, i.e, Gal-
207 Ura, compared to the control **(Supplementary Fig S2b).**
208 We further checked whether our mutants show protein aggregation under confocal microscopy.
209 For the microscopy, cultures were inoculated in SD-Ura, on the following day. After raffinose
210 wash and addition of 20% Galactose, we find two morphologies in confocal microscopy:
211 diffuse cytoplasmic and punctae forms. In TDP-43 and FUS, we find more punctae, indicating
212 protein aggregation in the yeast cell, and in control, we observe diffuse cytoplasmic signal,
213 which indicates no protein aggregation in the cell **(Supplementary Fig S2c).**
214 Since, TDP-43 and FUS mutant strains show a slow growth phenotype and aggregation of
215 proteins compared to control, we further checked these mutants against 38 DnaJ domain
216 chaperones to determine, how it enhances or rescues growth and aggragation properties.
217

218 **2.2 Classification of enhancers and suppressors of TDP-43 and FUS-*Drosophila* DnaJ**
219 **domain chaperones, based on growth assay**

220 We transformed 38 DnaJ domain chaperones ALS mutants, TDP-43 and FUS. These
221 transformed colonies of DnaJ domain chaperones were selected and inoculated in the SD-Trp-
222 Ura medium. On the second day, cultures were spotted onto SD-Trp-Ura and SGal-Trp-Ura
223 plates. SD-Trp-Ura is the control, and SGal-Trp-Ura serve as a test. Chaperones that enhance
224 the effect of the mutation are collectively called enhancers. Enhancers are those whose growth
225 are reduced in comparison to control TDP-43 and FUS. Since the plasmids are galactose
226 inducible, we find that chaperones CG2911, CG2790 and CG8476 grow slower on SGal-Trp-
227 Ura plates than control TDP-43; hence, these are enhacers of TDP-43 toxicity (**Fig. 1a).**
228 Chaperones Hsc20, CG2911, JdpC grow slower in SGal-Trp-Ura plates than in FUS with
229 empty vector strain. These chaperones are enhancers of FUS (**Fig. 1f).**

230 Chaperones that made the ALS mutants grow better in SGal-Trp-Ura plates than control, i.e.,
231 luciferase suppresses the effect of the ALS mutation, and are referred to as suppressors.
232 Chaperones Mrj, Hsc70-4, and CG7872 are suppressors of TDP-43 toxicity (**Fig.1a).** In the
233 SD-Trp-Ura plate, they serve as control **(Supplementary Fig. S4a).** Chaperones CG5001
234 (previously published) (Deo et al., 2024), CG6693 and CG32641 grow better in SGal-Trp-Ura
235 plates than luciferase. These chaperones are suppressors of FUS toxicity (**Fig. 1f).** SD-Trp-
236 Ura plates shows no difference in growth **(Supplementary Fig. S5a).**
237 To quantify the growth effect, we did a 48-hour growth curve assay of DnaJ chaperones on
238 TDP-43 and FUS mutants. TDP-43 and FUS transformants were inoculated in an SD-Trp-Ura
239 medium for primary culture. The following day, O.D. was adjusted, and 20% galactose was
240 added. Cultures were added in triplicate in a 96-well plate and placed in a Biotek Epoch
241 spectrophotometer for 48 hrs at 30°C for occasional shaking. The data obtained from this
242 experiment were processed in GraphPad Prism 8.0. Similar to the spot dilution assay,
243 This 48-hour growth curve shows a growth difference compared to the luciferase.
244 Chaperones CG2911, CG2790, and CG8476 grows slower than control in a 48-hour growth
245 curve. This indicates that these chaperones enhance the toxicity of mutant TDP-43. Chaperones
246 Mrj, Hsc70, and CG7872 grow better than control, suggesting these chaperones rescue TDP-
247 43 toxicity (**Fig. 1 b)**.
248 In FUS, chaperones Hsc20, CG2911, CG7130, and JDPC in presence of the FUS mutant grows
249 slower compared to luciferase. This indicates that these chaperones enhance the toxicity of
250 FUS. Co-expression of FUS with the chaperones CG6693, CG32641 and CG5001(Deo et al.,
251 2024) have been shown to rescue the slow growth phenotype (**Fig.1g).** In SD-Trp-Ura plates
252 there is no difference **(Supplementary Fig. S5a).**
253 For the classification of the enhancers and suppressors of DnaJ domain chaperones in the 48-
254 hour growth curve, we calculated the area under the curve based on the values of the 48-hour

growth curve. The area under the curve values were normalized with luciferase. A graph was plotted in GraphPad Prism 8.0. Positive values of chaperones on the right-hand side are considered suppressors. The negative values of chaperones on the left-hand side are called enhancers (**Fig. 1c and 1h).**

2.3 Classification of weak and ineffective enhancers of *Drosophila* DnaJ domain chaperones.

DnaJ domain chaperones of *Drosophila* were screened to see the effect on ALS mutant TDP-43 and FUS, after the yeast transformation of ALS mutants with DnaJ domain chaperones and co-chaperones. Initially, we checked by using a serial dilution assay. Positive clones were selected from the transformation and inoculated in SD-Trp-Ura (dextrose, YNB, and Tryptophan and Uracil lacking medium) (B. S. Johnson et al., 2008b). After 48 hrs, serially diluted cultures were spotted on SGal-Trp-Ura and SD-Trp-Ura plates. Plates with dextrose (SD) serve as a control **(Supplementary Fig. S4b and S5b)**, while galactose plates were observed for growth, as ALS plasmids have galactose-inducible promoters.

To quantify the effect of mutants on DnaJ domain chaperones, we did 48 hrs growth curve assay. ALS mutant TDP-43 and FUS with control luciferase and transformed chaperones were subjected to induced 20% galactose. These were grown at 30°C for 48 hrs, and the O. D_{600nm} with constant shaking, measured every 30 minutes. From 3 independent biological independent replicates, graphs were plotted in GraphPad Prism 8.0 software (**Fig.2b and 2g). The** red line shows the mutants with transformed DnaJ domain chaperones, and the blue line shows the growth curve of ALS mutants with empty vector. ($n=3$, $P<0.05$, paired t-test).

The area under the curves is calculated for each chaperone, including luciferase converted into logarithmic values. Each value was further normalized with luciferase. A graph was plotted in GraphPad Prism 8.0 software. Chaperones that grow slower with ALS mutants were aligned to

280 the right-hand side with a positive value were called suppressors, and the chaperones that were
281 aligned to the left-hand side with a negative value are called enhancers (**Fig.2c and 2h).** The
282 classification of enhancers and suppressors of other chaperones is based on the values of the
283 growth curve obtained from area under the curve.
284 In serial dilution assay and 48 hrs growth curve of TDP-43, chaperones CG12020, CG7394,
285 CG4164, DnaJ60, CG3061, Hsp70Aa, CG32641, DnaJ1, JdpC, CG2887, Hsc20 and JdpA,
286 grow less in comparison to the control. These are classified as weak enhancers. Other
287 chaperones like CG14650, Tpr2, CG9828, CG7556, P58IPK, and Hsp70Bb grow equally to
288 Luciferase and show no effect on the growth (n=3, $P<0.05$, paired t-test) shown in (**Fig. 2a).**
289 In serial dilution assay and 48 hrs growth curve of FUS, chaperones CG9828, CG12020,
290 Hsp70Aa, Hsp70Bb, CG11035, CG3061, DnaJ60, CG7133, CG14650, CG2887, CG10375
291 grow less compared to luciferase, are classified as weak enhancers, whereas chaperones
292 CG7556, CG17187, CG43322, Csp, Sec63, CG11035, and Hsc70-1 show no effect on growth
293 in the growth curve (**Fig. 2f).**

294 The area under the curve of TDP-43, chaperones CG10565, CG12020, CG3061, DnaJ1,
295 CG2911, CG7133, CG4164, DnaJ60, Droj1, and CG7394, JdpA, and JdpC are aligned to the
296 left-hand side. These are classified as weak enhancers **(Fig.2c)**. Whereas chaperones
297 CG14650, Tpr2, CG9828, CG7556, P58IPK, and Hsp70Bb show no significant effect on
298 growth. They are either aligned to the right-hand side or left-hand side and may be classified
299 as intermediate.

300 The area under the curve of FUS, chaperones CG9828, CG12020, Hsp70Aa, Hsp70Bb,
301 CG11035, CG3061, DnaJ60, CG7133, CG14650, CG2887, and CG10375 are aligned to the
302 left-hand side and assigned a negative value. These are called weak enhancers **(Fig.2h).**
303 Chaperones CG7556, CG17187, CG43322, Csp, Sec63, CG11035, P58IPK, and Hsc70-1 show

304 no effect on growth in the 48-hour growth curve. They are aligned either to the left-hand side
305 or the right-hand side. Therefore, they are classified as having no effect.
306

307 **2.4 Enhancers and suppressors of ALS mutant TDP-43 and FUS based on protein**
308 **aggregation in *S. cerevisiae***

309 Transformants of TDP-43 and FUS were induced with 20% galactose to express the ALS gene.
310 Under confocal microscope, GFP expression is observed in yeast cells (B. S. Johnson et al.,
311 2008b). TDP-43 and FUS showed puncta, a sign of protein aggregation, and the control showed
312 diffuse cytoplasmic pattern with no protein aggregation inside the cell.
313 Around 100-120 cells were counted for ALS mutant TDP-43, FUS, and control independently.
314 These were scored for the percentage of punctae and diffuse cytoplasmic GFP expression.
315 Representative images are shown in (**Fig.1d and 1i).** Based on confocal images, cells were
316 classified into two types: cells with diffuse cytoplasmic expression and then with punctae.
317 These were then compared to mutants with empty vector strains. The graph was plotted in
318 GraphPad Prism. Chaperones, when overexpressed with mutant, have a higher expression of
319 the cytoplasmic GFP diffusion than punctae. These chaperones are termed suppressors of the
320 mutation. Those chaperones that showed greater number of punctae than diffuse cytoplasmic
321 pattern was classified as enhancers. Chaperones Mrj, Hsc70-4, and CG7872 suppressed the
322 effect of the mutation, and chaperones CG2911, CG2790, and CG8476 enhanced the mutation
323 of TDP-43 in ALS (**Fig.1e and Table 2)**. Chaperones CG5001(previously published) and
324 CG6693 suppressed the effect of FUS toxicity, and chaperones Hsc20, CG2911, CG7130, and
325 JdpC enhanced the FUS toxicity in the yeast cells (**Fig. 1i and Table 4**).
326

327 **2.5 Classification of weak enhancers and no effect. Based on protein aggregation in TDP-**
328 **43 and FUS**

329 To check the protein aggregation of FUS and TDP-43 with the DnaJ domain chaperone,
330 microscopy was done. Transformed cultures were inoculated in an SD-Trp-Ura medium
331 (Dextrose, YNB, and Trp-Ura dropout). After 20% galactose induction, microscopy was done.
332 Chaperones that show more of the diffuse cytoplasmic signal than punctae are called
333 suppressors (CG10565, CG12020, CG3061, DnaJ1, CG2911, CG7133, CG4164, DnaJ60,
334 Droj1). Strains with chaperones CG7394, JdpA, and JdpC on the other hand, show more
335 punctae than diffuse cytoplasmic expression are the enhancers.
336 Microscopic images of TDP-43 with chaperones CG14650, Tpr2, CG9828, CG7556, P58IPK,
337 and Hsp70Bb have more punctae compared to luciferase. These chaperones show mixed
338 phenotype **(Fig.2d).**
339 Microscopic images of FUS with chaperones CG9828, CG12020, Hsp70Aa, Hsp70Bb,
340 CG11035, CG3061, DnaJ60, CG7133, CG14650, CG2887, and CG10375 show more of the
341 punctae than control. Chaperones CG7556, CG17187, CG43322, Csp, Sec63, CG11035,
342 P58IPK, and Hsc70-1 shows mixed phenotype (**Fig.2i).**
343 For the quantitation of microscopic data, 100 cells were counted. Punctae and diffuse
344 cytoplasmic morphology were counted for each transformant, and average values were plotted
345 in GraphPad prism **(Fig.2e and 2j).** Quantitation of both TDP-43 and FUS is given in Tables
346 3 and 5.
347 Chaperones of TDP-43, CG12020, CG7394, CG4164, DnaJ60, CG3061, Hsp70Aa, CG32641,
348 DnaJ1, JdpC, CG2887, Hsc20 and JdpA have a higher percentage of punctae than diffuse
349 cytoplasmic expression. Chaperones CG14650, Tpr2, CG9828, CG7556, P58IPK and
350 Hsp70Bb show a mixed phenotype.
351 Chaperones of FUS, CG9828, CG12020, Hsp70Aa, Hsp70Bb, CG11035, CG3061, DnaJ60,
352 CG7133, CG14650, CG2887, and CG10375 have a higher content of punctae compared to

353 luciferase. Chaperones CG7556, CG17187, P58IPK, CG43322, Csp, Sec63, CG11035,
354 CG10565 and Hsc70-1 shows a mixed phenotype.
355
356 **3.0 Discussion**
357 RNA-binding proteins TDP-43 and FUS plays a role in ALS pathogenesis. Both have some
358 structural similarities, including the presence of a RNA-binding domain and a prion-like
359 domain. They are both mutated in ALS (Gitler & Shorter, 2011a; Lagier-Tourenne et al., 2010).
360 Although they have certain structural similarities, both genes contribute independently to ALS
361 pathogenesis (Kwiatkowski et al., 2009b).
362 As per Arai and Newmann 2006, TDP-43 is localized in the nucleus and later spreads out to
363 form cytoplasmic aggregates in ALS and FTLD patients (Arai et al., 2006; Neumann et al.,
364 2006b).
365 Yeast cells do not have a true TDP-43 homolog but have RNA-binding proteins of similar
366 architectural domain. TDP-43 might aggregate and sequester these proteins, which will offset
367 their normal function [(Gitler & Shorter, 2011b).
368 In Parkinson's, Huntington's, Alzheimer's, and prion-related studies, the respective protein
369 forms, intracellular aggregates, and toxicity in yeast cells. Similarly, TDP-43 also forms
370 cytoplasmic aggregates and can be added to the list of human misfolding diseases of proteins
371 (Gitler, 2008).
372 FUS also forms cytoplasmic aggregates in neurons after a missense mutation (Vance, Rogelj,
373 Hortobágyi, et al., 2009). FUS is normally located in the nucleus. After mutation, FUS forms
374 pathogenic aggregates in motor neurons (Ju et al., 2011)
375 *In vitro studies* from yeast show TDP-43 and FUS tends to form cytoplasmic aggregates
376 (Elden et al., 2010b; B. S. Johnson et al., 2008b, 2009). In animals and cellular models ATX2
377 gene is found to contribute to TDP-43 toxicity and ALS pathogenesis. It is a polyglutamine

378 protein, and the human orthologue of yeast found mutated in spinocerebellar ataxia type 2
379 (Lorenzetti et al., 1997). Furthermore, it was observed that TDP-43 and ATX2 are associated
380 in a complex (Elden et al., 2010b). In yeast, the pure form of the TDP-43 gene *in vitro* can form
381 multiple aggregates *in vivo*. Additionally, a pure TDP-43 aggregates assay aids in identifying
382 small molecules and cellular factors capable of impeding or reversing TDP-43 aggregates (B.
383 S. Johnson et al., 2009). After dissecting the TDP-43 and expressing it in yeast, it was noticed
384 that the C-terminal and RNA recognition motif contribute to TDP-43 toxicity (B. S. Johnson et
385 al., 2008a).
386 Yeast is a genetically tractable model, and it is possible to reiterate multiple features of TDP-
387 43 pathology in yeast (Gitler, 2008).This includes screening of multiple genomes for detecting
388 modifications of protein aggregation and their toxicity. This is one approach that can be used
389 for effective diagnosis and treatment (B. S. Johnson et al., 2008a).
390 In our observations, TDP-43 and FUS mutants showed slow growth in yeast cells after serial
391 dilution, indicating cellular stress [(B. S. Johnson et al., 2008b; Sun et al., 2011). After 24 hours
392 of galactose induction, these mutants show aggregates in the cell under the microscope.
393 Screening of these mutants with 38 DnaJ domain chaperones showed that some of the
394 chaperones enhanced and others reduced the toxicity of the mutants in ALS. We labelled them
395 as enhancers and suppressors of TDP-43 and FUS respectively.
396 By screening *Drosophila* DnaJ domain chaperones, we found that chaperones CG7872, Mrj,
397 and Hsc70-4 can rescue the toxicity of mutant TDP-43. HSc70-1 slightly rescues the toxic
398 phenotype of TDP-43 to a great extent. Hsc70-4. CG32641 and CG6693 suppresses the toxicity
399 of mutant FUS. Previous reports show that, CG5001 rescues both the mutants TDP-43 and
400 FUS (Deo et al., 2024). Human homologues of Hsp70, chaperones DNAJAs, DNAJBs, and
401 DNAJCc chaperones rescue the toxicity of TDP-43 in ALS (Barbieri et al., 2025).

From our studies we see, chaperone CG2911 acts as a common enhancer for both TDP-43 and FUS.

Chaperones CG7872, Hsc70-4, and Mrj demonstrate a more significant growth effect in mutant TDP-43. In the serial dilution assay and the growth curve, they grow comparatively better than the control. In microscopy, they exhibit a higher prevalence of diffuse cytoplasm morphology than punctae; hence, we refer to them as suppressors of TDP-43.

DnaJ chaperone Mrj is present ubiquitously in the cytosol. Mrj's human orthologue, DNAJB6, is known for its potent anti-aggregation effect in mouse models (Kakkar et al., 2016). A mutation in the human DNAJB6 (Mrj) causes frontotemporal dementia and limb-girdle muscular dystrophy type 1 case of the patient's brain sample (Yabe et al., 2014). It was also found that DNAJB6 inhibits polyQ aggregation and increases the life span in polyQ mice (Kakkar et al., 2016). *Drosophila* Mrj helps Orb2 to reduce its prion conversion and also helps reduce Htt aggregates (Desai et al., 2024). DNAJC25 is an ortholog of CG7872, belonging to the HSP40 family C, and plays a vital role in various human diseases, including neurodegenerative disorders (LIU et al., 2012b). Co-chaperone Hsc70 influences TDP-43 toxicity in ALS patients (Arosio et al., 2020)

Hsc70-4 is the human orthologue of HPSA8 and has been found to control multiple studies of autophagy (Braell et al., 1984; Stricher et al., 2013). Previously, it was also found to prevent necroptosis initiation and bind to reverse RIP3 amyloid in mammalian cell culture(Wu et al., 2023)

In the FUS mutants, chaperones CG32641 and CG6693 come up as suppressors as they showed better growth than luciferase in both serial dilution and growth curve. Microscopic quantitation shows more of the diffuse cytoplasmic morphology and fewer punctae in the cell. Therefore, they are referred to as suppressors of FUS toxicity.

Reports show show that DNAJC9 is the human orthologue of CG6693 and is associated with cervical cancer. It is probably upregulated by reducing or protecting against apoptosis in the cancer cell line (Incekara & Acun, 2023). Studies in zebrafish stated that DNAJC9 acts in the downstream regulating pathway of the tumor suppressor gene p53 (Mandriani et al., 2016). Also, CG32641 has a DNAJB9 human orthologue and is known for its ER-associated degradation machinery (Lai et al., 2012). In the mouse model, it was found that it rescues cystic fibrosis-causing gene Δ F508, and also directly interacts with CFTR (Huang et al., 2019).

From the studies of Drosophila DnaJ domain chaperones, we also discovered certain enhancers that exacerbate the toxic phenotype, specifically slow growth and aggregation in both mutant FUS and TDP-43. Chaperones CG2911, CG2790, and CG8476 enhance TDP-43 toxicity and have also been shown to be toxic in multiple studies. DNAJC21 is the human orthologue of CG2790, and its mutation is associated with bone marrow failure and cancer (Tummala et al., 2016). DNAJB9, is the human orthologue of CG8476, whose normal function involves protein folding. It is predominantly active in the endoplasmic reticulum and is found in the miR-32 gene in myeloid acute leukaemia (Thomson & Dinger, 2016).

Whereas, chaperones Hsc20, CG2911, CG7130, and JDPC are enhancers of mutant FUS. They also have a role in other disorders like Hsc20 which is also a mitochondrial chaperone, its human orthologue is HSCB; Mutation of Hsc20 in *Drosophila* larvae causes reduced iron-sulphur cluster enzyme activity (Uhrigshardt et al., 2013). JdpC has a human orthologue to DNAJC12, and in whole-exome sequencing, it is found responsible for hyperphenylalaninemia and global developmental delay in some children (Veenma et al., 2018).

CG2911 acts as an enhancer for in both TDP-43 and FUS. Its human orthologue is DNAJC24, which recently was reported to be involved in hepatocellular carcinoma (D. Liu et al., 2024). In our studies, it also shows toxicity when overexpressed in both mutants of TDP-43 and FUS.

While screening in the TDP-43 background we found that chaperones CG12020, CG7394, CG4164, DnaJ60, CG3061, Hsp70Aa, CG32641, DnaJ1, JdpC, CG2887, Hsc20 and JdpA are weak enhancers. This can be attributed to the slow growth phenotype of these chaperone in comparison to the mutant. In image analysis, accordingly, we labelled them as weak enhancers **[Table.1 (Fig. 2a, 2b**, **2c, and 2e)]**.

In the FUS strains, chaperones CG9828, CG12020, Hsp70Aa, Hsp70Bb, CG11035, CG3061, DnaJ60, CG7133, CG14650, CG2887, and CG10375 are weak enhancers. Their growth and spot dilution assay show slower growth compared to luciferase. Also, in microscopy, they show more puncta than luciferase. In the area under the curve graph, they are aligned on the left-hand side, and in microscopic quantitation, they show more puncta. Therefore, they are classified as the weak enhancers of FUS toxicity **[Table.1** (**Fig.2f, 2g, 2h, and 2i)].**

Some chaperones do not show any significant change in the toxicity of mutant TDP-43 example, CG14650, Tpr2, CG9828, CG7556, P58IPK, and Hsp70Bb. Serial dilution and growth curve results show equal growth. It is difficult to conclude whether they are enhancers or suppressors.

Similarly, in FUS mutants some chaperones, CG7556, CG17187, P58IPK, CG43322, Csp, Sec63, CG11035, CG10565, and Hsc70-1 do not show significant effects in spot dilution and growth curve. From these data, it is difficult to conclude whether these chaperones have any effect on FUS toxicity.

In both the mutant TDP-43 and FUS, Hsc70Aa and Hsc70Bb chaperone have no effect or weak enhancer.

In our study, we used *Drosophila* DnaJ domain chaperones in an yeast background to look for potential suppressors and enhancers in both TDP-43 and FUS. Also, we find suppressors and enhancers that were previously unknown in ALS.

474 Based on the *Drosophila* DnaJ domain chaperone screening with FUS and TDP-43 mutants,
475 we find that chaperone CG7872 reduces the toxicity of TDP-43 in yeast cells, which is
476 previously unknown. There are many studies on Mrj, which show that it reduces the toxic
477 aggregation in Huntington's and Parkinson's disease (Aprile et al., 2017; Desai et al., 2024;
478 Kakkar et al., 2016). Based on our findings, we think Mrj possibly reduces the toxicity in ALS
479 in a yeast model. Co-chaperone Hsc70 is found to reduce the toxic TDP-43 aggregation in
480 sporadic ALS patients (Arosio et al., 2020).
481 We also find that chaperones CG32641 and CG6693 rescus the toxicity of FUS in yeast cells,
482 which was not reported previously.
483 The hypothetical model in **Fig.3** shows the mechanism of action.
484 In this study, we have used a cloned library of 38 DnaJ domain chaperones of flies and
485 expressed them in two ALS mutants, TDP-43 and FUS. This will help shed some light on the
486 differences and similarities in the pathways regulated by TDP-43 and FUS in controlling the
487 pathogenesis of ALS.
488

489 **4.0 Material and Methods**

490 **4.1 Cloning of DnaJ domain chaperones and co-chaperones (Hsp40, Hsc70, and Hsp70)**
491 **library in yeast**

492 *Drosophila* Hsp40 and Hsp70 proteins were cloned by the Topo-D-Entr cloning kit (Invitrogen)
493 into the Topo-D-Entr vector. This was done post-PCR amplification using gene-specific
494 primers. Constructs were confirmed by sequencing and were transferred to the destination
495 vector pUASgHA for Hsp40 (Bischof et al., 2013; Joag et al., 2020; Warrick et al., 1999) and
496 pUASt-ccdB-FLAG (pTWF) for Hsp70.
497 For expression of Hsp40 and Hsp70 in yeast cells, Topo-D-Entr clones were cloned in the
498 destination vector pAG424GALccdB-HA with a 3X HA tag at the C-terminal (Hageman et al.,

2011). The protein expression of each isoform was confirmed by immunoblotting using either an anti-HA antibody or an anti-FLAG antibody accordingly (Desai et al., 2024) .

4.2 Construction of yeast overexpression of DnaJ chaperones and co-chaperones in yeast TDP-43 and FUS strain backgrounds

4.2.1 Bacterial Transformation

For the bacterial transformation, DH5αCells were made competent by using the calcium chloride method. 200µl competent cells were taken, and 1 µl plasmid DNA of ALS plasmids pRS426 Gal-TDP-43-GFP and pAG416 Gal-FUS-YFP were added. These were incubated on ice for 30 minutes. Then, heat shock was given for 2 minutes at 42°C, and it was kept on ice for 1 minute. Luria Broth was added to it, and incubated at 37°C for 30 to 45 minutes. The cells were centrifuged at 8000 rpm for 3 minutesat room temperature. Then, the supernatant was discarded, and the cells were resuspended in 200 µl of Luria broth. They were plated with glass beads on LB amp plates, and finally, the plates were incubated overnight (maximum 18 hours) at 37°C. These plasmids were deposited by Aaron Gilter lab, numbered 27467 and 29592, respectively(B. S. Johnson et al., 2008a; Sun et al., 2011) .

4.2.2 Plasmid Isolation

A single colony of transformed bacteria was inoculated in 5ml LB broth, and 5µl of Ampicillin was added and kept in a 37°C shaker overnight. The culture was centrifuged at 10,000 rpm for 5 minutes, and of GET was added. The culture was incubated on ice for 2 minutes. 200µl of alkaline SDS was added to it. The mixture was incubated on ice for 2 minutes, and 150µl acidic KoAc and incubated again on ice for 5 minutes. The whole culture was centrifuged at 14,000 rpm for 5 minutes at 4°C. The supernatant was collected, and 400µl of phenol: chloroform solution was added. It was centrifuged at 14,000 rpm for 5 minutes at 4°C. The aqueous phase was collected, and 1 mL of 100% ethanol was added to it. This was kept at -20°c for 15 minutes for precipitation and centrifuged at 14,000 rpm for 10 minutes at 4°C. The supernatant was

decanted, and the pellet was washed with 500µl of 70% ethanol by centrifuging it at 14,000 rpm for 5 minutes at 4°C. The supernatant was discarded, and the pellet was air-dried. Once dried, the pellet was resuspended in 50µl of TE buffer. Finally, the plasmid was stored at -20°C.

4.2.3 Yeast Transformation

Yeast strain *Saccharomyces cerevisiae* (w303a, MATa, ade2, his3, leu2, trp1, ura3) cells were grown in YPD (yeast extract, peptone, and dextrose) medium, i.e., Primary culture, and allowed to grow overnight at 30°C, till mid log phase. After spinning down the cells at 5000 rpm for 5 minutes at room temperature, the pellet was resuspended in autoclaved distilled water to wash off residual media. The pellet was resuspended completely after spinning down in 100mM LiOAc, from which aliquots were made as per the number of transformations to be performed. Cells were centrifuged, and to each vial, 50% Polyethylene Glycol, 1 M Lithium acetate, ss DNA, and plasmid DNA were added (Ito et al., 1983). The cell suspension was vortexed to ensure resuspension and subjected to a heat shock at 42°C for 45 minutes in a water bath. The cell suspension was centrifuged at 5000 rpm for 5 min at room temperature, and autoclaved distilled water was used to resuspend the pellet.

The plasmids TDP-43 (pRS426 Gal-TDP-43-GFP) and FUS (pAG416 Gal-FUS-YFP) are galactose inducible and have an Uracil marker and are placed on SD-Ura, having a mixture of Sucrose, YNB, and amino acid lacking mixture Uracil. The media used were from Clontech Laboratories. USA. The plates were incubated at 30°C for 3-4 days (Gietz & Schiestl, 2007).

In case of the DnaJ domain chaperone, double transformation was done with ALS mutants. These chaperones have a Trp marker. Transformation was done on SD-Trp-Ura (YNB, dextrose, agar, and amino acid mixture lacking Tryptophan and Uracil) medium.

4.2.3 Serial dilution assay

A single colony was inoculated with the transformed cultures of TDP-43 and FUS in 500µl of media of SD-Ura and allowed to grow overnight on a shaking incubator at 30°C. Raf-Ura (YNB, raffinose and amino acid mixture lacking Tryptophan and Uracil) washes were given, i.e., dextrose in the medium was replaced by raffinose, and their $O.D_{600}$. was adjusted to 0.2 and allowed to grow again in the same conditions. Following day, the O.D was adjusted to 0.2, and the culture was diluted up to 1/10000th dilution (10^0 to 10^{-5}dilutions) and 3-6 µl of each dilution was spotted on to SD-Ura and SGal-Ura (galactose, YNB, Agar and amino acid mixture lacking Tryptophan and Uracil) plates and incubated at 30^0C for 2-4 days, as all the plasmids used are galactose inducible.

For the double transformation of ALS mutant strains, two clones were selected and inoculated into an SD-Trp-Ura medium. Further plated on SD-Trp-Ura and SGal-Trp-Ura plates with control luciferase.

4.2.4 Growth Assay

Transformed colonies of double transformants were inoculated in SD-Trp-Ura (Sucrose, YNB, and amino acid lacking mixture Uracil) medium overnight on a shaking incubator at 30°C. The next day, Raf-Trp-Ura (Raffinose, YNB, and amino acid lacking mixture Tryptophan Uracil) washes were given, and their $O.D_{600}$. was adjusted to 0.2 and 20% galactose was added to each culture of Raf-Trp-Ura and these were added to 96 well plates in triplicates with blank (Raf-Trp-Ura + Gal). 96-well plate was placed in an Epoch2 BioTek Spectrophotometer for 48 hours at 30°C with continuous orbital shaking, and $O.D_{600}$. was measured every 30 min. The data obtained after 48 hrs were plotted in GraphPad software, and the Growth curve was plotted for each culture.

4.2.5 Microscopy

By using confocal microscopy, we analysed the protein aggregation status of the yeast cells as the FUS and TDP43 constructs had a GFP tag.All transformed *S. cerevisiae* strains were grown

overnight in SD-Trp-Ura broth at 30°C. The next day, they were subjected to Raf-Trp-Ura$^-$ wash for the removal of residual dextrose. O.D$_{600}$ was adjusted to 0.2 in Raf-Trp-Ura$^-$. After 2-3 hours, they were induced with 20% galactose. The next day, they were centrifuged and resuspended in the residual media, and a smear was prepared and observed under a confocal microscope under a 60x objective and GFP laser. Images were processed using Fiji software.

4.2.5 Quantitation of Image Analysis

Mutant strains transformed with different chaperones displayed two different morphologies, punctae and diffuse cytoplasmic signal. These were counted in 3 biological replicates for each strain. Chaperones that show more of the diffuse cytoplasmic expression and fewer punctae compared to luciferase are classified as suppressors, and chaperones that show a greater number of punctae and less of the diffuse cytoplasmic signal are classified as enhancers.

5.0 Acknowledgment

We would like to thank Amitabha Majumdar for providing the plasmids and the instrument setup required for this study. We would like to thank Meghal Desai for the plasmid library construction.

This work was supported by research grants from the Department of Biotechnology (DBT-IYBA) (BT/09/IYBA/2015/03) and the DBT RLS (BT/RLF/Re-entry/54/2013) to TB . SA recipients of the Indian Council of Medical Research (ICMR) senior research fellowship (SRF) **(**5/3/8/89/ITR-F/2020-ITR).

.

6.0 Authors contribution

The experiments are designed in this study by TB. The manuscript was written by SA and TB. Experiments were done by SA.

7.0 Declaration of Interest

Conflict of interest: The authors declare no conflict of interest.

8.0 Declaration of generative AI in scientific writing

No generative AI is used during scientific writing

9.0 Figure Legends

Fig.1 Effect of DnaJ domain chaperones on the growth of ALS mutant TDP-43:

a. DnaJ domain chaperones transformed with ALS mutant TDP-43 were serially diluted and spotted onto SD-Trp-Ura and SGal-Trp-Ura plates. In this figure, SGal-Trp-Ura was shown as a test with TDP-43, and luciferase was used as a control.

b. 48hrs growth curve of DnaJ domain chaperone transformed with TDP-43 mutant. Three independent biological replicates were used (n=3, $P<0.001$, paired t-test). The blue line indicates mutant TDP-43 with luciferase as control, and the red line indicates the DnaJ domain chaperones with the TDP-43 mutant.

c. Enhancers and suppressors of TDP-43 mutant plotted, based on the area under the curve values obtained from the growth curves using GraphPad Prism software. The area under the growth curve values are converted into a logarithmic scale and normalized. Chaperones on the right-hand side are the suppressors, and those on the left-hand side are enhancers.

Fig.1 Effect of DnaJ domain chaperones on protein aggregation phenotype of the TDP-43 mutant of ALS

618 **d.** Microscopic images showing protein aggregation and diffuse cytoplasm phenotype in the
619 *Saccharomyces cerevisiae* model of ALS. TDP-43 aggregates are seen in the form of bright
620 GFP punctae after induction with 20% Galactose.

621 **e**. Two different morphologies exhibited by the different DnaJ domain chaperones with the
622 TDP-43 mutant. 100-120 cells were counted for each chaperone. The average score was
623 plotted using GraphPad prism. Table of total diffuse cytoplasmic signal and punctae.

624 **Table 2** shows the quantification of punctae and diffuse cytoplasmic signal of 7 DnaJ domain
625 chaperones

626 **Fig.2 Effect of growth on ALS mutant due to chaperones (Serial dilution assay on**
627 **Galactose medium)**

628 **a**. Representative image of serial dilution assay on SGal-Trp-Ura medium of DnaJ chaperones
629 and co-chaperones mentioned in the study.

630 **b. Effect of chaperones on the growth of ALS mutant TDP-43 (48-hour growth curve)**

631 48-hr growth curve of the remaining 19 DnaJ domain chaperones with Luciferase. Data
632 shown in **Figure 2b** were obtained from three independent biological replicates (n=3, $P<0.05$,
633 paired t-test)

634 **c.** Enhancer and suppressor classification of the 19 DnaJ domain chaperones with TDP-43
635 mutant based on area under the curve values derived from GraphPad Prism. The area under
636 the curve values of each chaperone were converted to a logarithmic scale and normalised. It
637 is plotted via GraphPad Prism and the area under the curve values of the graph on the right-
638 hand side are the suppressors, and those on the left-hand side are the enhancers.

639 **d. Effect of chaperones on protein aggregation phenotype of TDP-43 mutant.**

640 19 different DnaJ chaperones and co-chaperones showing protein aggregation in the yeast
641 model of ALS. Following induction with 20% galactose, microscopic images were taken.
642 TDP-43 appeared as bright GFP punctae.
643 **e.** Graph of 19 chaperones plotted in Graphpad Prism shown in Figure **2c**. For each
644 chaperone, 100-120 cells were counted, and the average was plotted.

645 **Table 3** shows the quantification of punctae and diffuse cytoplasmic signal of 19 DnaJ
646 domain chaperones

647 **g.** DnaJ domain chaperones transformed with ALS mutant FUS was serially diluted and
648 spotted onto SD-Trp-Ura and SGal-Trp-Ura plates. In this figure, SGal-Trp-Ura was shown as
649 a test with FUS luciferase as a control.

650 **h**. 48-hour growth curve of DnaJ domain chaperone transformed with FUS mutant. Data from
651 three independent biological replicates were collected (n=3, P<0.001, paired t-test). The blue
652 line indicates mutant FUS with luciferase as control, and the red line indicates DnaJ domain
653 chaperones with the FUS mutant.

654 **i**.Enhancers and suppressors of FUS mutant based on the area under the curve values of
655 obtained from the growth curves using GraphPad Prism software. The area under the growth
656 curve values are converted into logarithmic scale and normalized. Chaperones on the right-
657 hand side are the suppressors, and on the left-hand side, chaperones are enhancers

658 **j.** Microscopic images showing protein aggregation and diffuse cytoplasm phenotype in the
659 *Saccharomyces cerevisiae* model of ALS. FUS aggregates are seen in the form of bright GFP
660 punctae after induction with 20% Galactose.

661 **k**.Two different morphologies exhibited by the different DnaJ domain chaperones with the
662 FUS mutant. Counted 100-120 cells for each chaperone average was plotted on GraphPad
663 Prism.

664 **Table 4** shows the quantification of punctae and diffuse cytoplasmic signal of 6 DnaJ
665 domain chaperones

666 **Fig.2 Effect of growth on ALS mutant FUS due to chaperones (Spot dilution assay on**
667 **Galactose medium)**

668 **f**. Representative image of serial dilution assay on SGal-Trp-Ura medium of DnaJ chaperones
669 and co-chaperones with the FUS mutant mentioned in this study shows a weak enhancer, and
670 some show no effect.

671 **g.** 48-hour growth curve of DnaJ domain chaperone transformed with FUS mutant. Three
672 biological replicates of data were collected (n=3, P<0.001, paired t-test). The blue line
673 indicates mutant FUS with control Luciferase, and the red line indicates DnaJ domain
674 chaperones with the FUS mutant described as a weak enhancer, and some show no effect on
675 the mutant FUS

676 **h**. Enhancer and suppressor classification of the remaining 21 DnaJ domain chaperones with
677 FUS mutant, based on the area under the curve values derived from GraphPad Prism. The
678 area under the curve values of each chaperone were converted to a logarithmic scale and
679 normalized. It is plotted via GraphPad Prism and the area under the curve values graph on the
680 right-hand side are the suppressors, and those on the left-hand side are the enhancers.

681 **Fig 2. Effect of DnaJ domain chaperones on the protein aggregation phenotype of the**
682 **FUS mutant of ALS.**

683 **f.** Different DnaJ chaperones and co-chaperones are showing protein aggregation in the yeast
684 model of ALS. following 20% galactose, microscopic images were taken protein
685 aggregation was seen in the form of bright GFP punctae, indicating the weak enhancer. Some
686 chaperones show both diffuse cytoplasmic signal and punctae phenotype as per the growth

687 assay, and microscopic analysis indicates they are either enhancers or suppressors and do not
688 show a strong effect on the mutant FUS.

689 **g**. Graph of 21 chaperones plotted in Graphpad Prism is shown in Figure 2j. For each
690 chaperone, 100-120 cells were counted, and the average was plotted.

691 **Table 5** shows the quantification of punctae and diffuse cytoplasmic signal of 21 DnaJ
692 domain chaperones

693

694 **Fig.3 Hypothetical model**

695 This schematic diagram is the overall hypothesis of our research, in which the ALS mutant
696 genes of TDP-43 and FUS, when mutated, form misfolded proteins, resulting in an
697 aggregation of protein within the cell. by interacting with Hsp40 chaperones, i.e, Drosophila
698 DnaJ domain chaperones with yeast cells, they either enhance the toxicity or rescue the
699 toxicity of these two mutants. Toxic phenotype in yeast represents puncta in the cytoplasm,
700 and rescue represents cytoplasmic diffusion.

701

702 **10. Tables**

TDP-43		FUS	
Weak enhancer	**No effect**	**Weak enhancer**	**No effect**
CG12020	CG14650	CG9828	CG7556
CG7394	Tpr2	CG12020	CG17187
CG4164	CG7556	Hsp70Aa	P58IPK
Dnaj60	CG9828	Hsp70Bb	Csp
CG3061	Hsp70Bb	CG11035	Sec63
Hsp70Aa	P58IPK	CG3061	CG43322
CG32641		Dnaj60	CG11035
DnaJ1		CG7133	Hsc70-1
JdpC		CG3061	CG10565
CG2887		CG14650	
Hsc20		CG2887	
JDPA		CG10375	

Table 1. List of weak enhancers and no effect chaperones on ALS mutant TDP-43 and FUS

11.0 References: -

1. Aprile, F. A., Källstig, E., Limorenko, G., Vendruscolo, M., Ron, D., & Hansen, C. (2017). The molecular chaperones DNAJB6 and Hsp70 cooperate to suppress α-synuclein aggregation. *Scientific Reports*, *7*(1), 9039. https://doi.org/10.1038/s41598-017-08324-z

2. Arai, T., Hasegawa, M., Akiyama, H., Ikeda, K., Nonaka, T., Mori, H., Mann, D., Tsuchiya, K., Yoshida, M., Hashizume, Y., & Oda, T. (2006). TDP-43 is a component of ubiquitin-positive tau-negative inclusions in frontotemporal lobar degeneration and amyotrophic lateral sclerosis. *Biochemical and Biophysical Research Communications*, *351*(3), 602–611. https://doi.org/10.1016/j.bbrc.2006.10.093

3. Armon, C. (2009). Smoking may be considered an established risk factor for sporadic ALS. *Neurology*, *73*(20), 1693–1698. https://doi.org/10.1212/WNL.0b013e3181c1df48

4. Arosio, A., Cristofani, R., Pansarasa, O., Crippa, V., Riva, C., Sirtori, R., Rodriguez-Menendez, V., Riva, N., Gerardi, F., Lunetta, C., Cereda, C., Poletti, A., Ferrarese, C., Tremolizzo, L., & Sala, G. (2020). HSC70 expression is reduced in lymphomonocytes of sporadic ALS patients and contributes to TDP-43 accumulation. *Amyotrophic Lateral Sclerosis & Frontotemporal Degeneration*, *21*(1–2), 51–62. https://doi.org/10.1080/21678421.2019.1672749

5. Barbieri, E. M., Linsenmeier, M., Whiteman, K. R., Cheng, Y., Braganza, S., Copley, K. E., Miranda-Castrodad, P., Lewis, B., Villafañe, K., Amado, D. A., Davidson, B. L., & Shorter, J. (2025). *Scouring the human Hsp70 network uncovers diverse chaperone safeguards buffering TDP-43 toxicity*. https://doi.org/10.1101/2025.05.10.653282

6. Bar-Lavan, Y., Shemesh, N., & Ben-Zvi, A. (2016). Chaperone families and interactions in metazoa. *Essays in Biochemistry*, *60*(2), 237–253. https://doi.org/10.1042/EBC20160004

7. Bascos, N. A. D., & Landry, S. J. (2019). A History of Molecular Chaperone Structures in the Protein Data Bank. *International Journal of Molecular Sciences*, *20*(24). https://doi.org/10.3390/ijms20246195

8. Beissinger, M., & Buchner, J. (1998). How chaperones fold proteins. *Biological Chemistry*, *379*(3), 245–259.

9. Bischof, J., Björklund, M., Furger, E., Schertel, C., Taipale, J., & Basler, K. (2013). A versatile platform for creating a comprehensive UAS-ORFeome library in *Drosophila*. *Development*, *140*(11), 2434–2442. https://doi.org/10.1242/dev.088757

10. Braell, W. A., Schlossman, D. M., Schmid, S. L., & Rothman, J. E. (1984). Dissociation of clathrin coats coupled to the hydrolysis of ATP: role of an uncoating ATPase. *The Journal of Cell Biology*, *99*(2), 734–741. https://doi.org/10.1083/jcb.99.2.734

11. Caplan, A. J. (2003). What is a co-chaperone? *Cell Stress & Chaperones*, *8*(2), 105–107. https://doi.org/10.1379/1466-1268(2003)008<0105:wiac>2.0.co;2

12. Carrell, R. W., & Lomas, D. A. (1997). Conformational disease. *Lancet (London, England)*, *350*(9071), 134–138. https://doi.org/10.1016/S0140-6736(97)02073-4

13. Cheetham, M. E., & Caplan, A. J. (1998). Structure, function and evolution of DnaJ: conservation and adaptation of chaperone function. *Cell Stress & Chaperones*, *3*(1), 28. https://doi.org/10.1379/1466-1268(1998)003<0028:SFAEOD>2.3.CO;2

14. Cirulli, E. T., Lasseigne, B. N., Petrovski, S., Sapp, P. C., Dion, P. A., Leblond, C. S., Couthouis, J., Lu, Y.-F., Wang, Q., Krueger, B. J., Ren, Z., Keebler, J., Han, Y., Levy, S.

E., Boone, B. E., Wimbish, J. R., Waite, L. L., Jones, A. L., Carulli, J. P., … Goldstein, D. B. (2015). Exome sequencing in amyotrophic lateral sclerosis identifies risk genes and pathways. *Science*, *347*(6229), 1436–1441. https://doi.org/10.1126/science.aaa3650

15. Couthouis, J., Hart, M. P., Shorter, J., DeJesus-Hernandez, M., Erion, R., Oristano, R., Liu, A. X., Ramos, D., Jethava, N., Hosangadi, D., Epstein, J., Chiang, A., Diaz, Z., Nakaya, T., Ibrahim, F., Kim, H.-J., Solski, J. A., Williams, K. L., Mojsilovic-Petrovic, J., … Gitler, A. D. (2011). A yeast functional screen predicts new candidate ALS disease genes. *Proceedings of the National Academy of Sciences*, *108*(52), 20881–20890. https://doi.org/10.1073/pnas.1109434108

16. De Jong, S. W., Huisman, M. H. B., Sutedja, N. A., van der Kooi, A. J., de Visser, M., Schelhaas, H. J., Fischer, K., Veldink, J. H., & van den Berg, L. H. (2012). Smoking, alcohol consumption, and the risk of amyotrophic lateral sclerosis: a population-based study. *American Journal of Epidemiology*, *176*(3), 233–239. https://doi.org/10.1093/aje/kws015

17. Deo, A., Ghosh, R., Ahire, S., Marathe, S., Majumdar, A., & Bose, T. (2024). Two novel DnaJ chaperone proteins CG5001 and P58IPK regulate the pathogenicity of Huntington's disease related aggregates. *Scientific Reports*, *14*(1), 20867. https://doi.org/10.1038/s41598-024-71065-3

18. Desai, M., Hemant, Deo, A., Naik, J., Dhamale, P., Kshirsagar, A., Bose, T., & Majumdar, A. (2024). Mrj is a chaperone of the Hsp40 family that regulates Orb2 oligomerization and long-term memory in Drosophila. *PLOS Biology*, *22*(4), e3002585. https://doi.org/10.1371/journal.pbio.3002585

19. Elden, A. C., Kim, H.-J., Hart, M. P., Chen-Plotkin, A. S., Johnson, B. S., Fang, X., Armakola, M., Geser, F., Greene, R., Lu, M. M., Padmanabhan, A., Clay-Falcone, D., McCluskey, L., Elman, L., Juhr, D., Gruber, P. J., Rüb, U., Auburger, G., Trojanowski, J. Q., … Gitler, A. D. (2010a). Ataxin-2 intermediate-length polyglutamine expansions are associated with increased risk for ALS. *Nature*, *466*(7310), 1069–1075. https://doi.org/10.1038/nature09320

20. Elden, A. C., Kim, H.-J., Hart, M. P., Chen-Plotkin, A. S., Johnson, B. S., Fang, X., Armakola, M., Geser, F., Greene, R., Lu, M. M., Padmanabhan, A., Clay-Falcone, D., McCluskey, L., Elman, L., Juhr, D., Gruber, P. J., Rüb, U., Auburger, G., Trojanowski, J. Q., … Gitler, A. D. (2010b). Ataxin-2 intermediate-length polyglutamine expansions are associated with increased risk for ALS. *Nature*, *466*(7310), 1069–1075. https://doi.org/10.1038/nature09320

21. Garcia-Toscano, L., Currey, H. N., Hincks, J. C., Stair, J. G., Lehrbach, N. J., & Liachko, N. F. (2024). Decreased Hsp90 activity protects against TDP-43 neurotoxicity in a C. elegans model of amyotrophic lateral sclerosis. *PLOS Genetics*, *20*(12), e1011518. https://doi.org/10.1371/journal.pgen.1011518

22. Gaudet, P., Livstone, M. S., Lewis, S. E., & Thomas, P. D. (2011). Phylogenetic-based propagation of functional annotations within the Gene Ontology consortium. *Briefings in Bioinformatics*, *12*(5), 449–462. https://doi.org/10.1093/bib/bbr042

23. Ghasemi, M., & Brown, R. H. (2018). Genetics of Amyotrophic Lateral Sclerosis. *Cold Spring Harbor Perspectives in Medicine*, *8*(5). https://doi.org/10.1101/cshperspect.a024125

24. Gietz, R. D., & Schiestl, R. H. (2007). High-efficiency yeast transformation using the LiAc/SS carrier DNA/PEG method. *Nature Protocols*, *2*(1), 31–34. https://doi.org/10.1038/nprot.2007.13

25. Gitler, A. D. (2008). Beer and Bread to Brains and Beyond: Can Yeast Cells Teach Us about Neurodegenerative Disease? *Neurosignals*, *16*(1), 52–62. https://doi.org/10.1159/000109759

26. Gitler, A. D., & Shorter, J. (2011a). RNA-binding proteins with prion-like domains in ALS and FTLD-U. *Prion*, *5*(3), 179–187. https://doi.org/10.4161/pri.5.3.17230

27. Gitler, A. D., & Shorter, J. (2011b). RNA-binding proteins with prion-like domains in ALS and FTLD-U. *Prion*, *5*(3), 179–187. https://doi.org/10.4161/pri.5.3.17230

28. Goedert, M. (2004). Tau protein and neurodegeneration. *Seminars in Cell & Developmental Biology*, *15*(1), 45–49. https://doi.org/10.1016/j.semcdb.2003.12.015

29. Gu, J., Liu, Z., Zhang, S., Li, Y., Xia, W., Wang, C., Xiang, H., Liu, Z., Tan, L., Fang, Y., Liu, C., & Li, D. (2020). Hsp40 proteins phase separate to chaperone the assembly and maintenance of membraneless organelles. *Proceedings of the National Academy of Sciences of the United States of America*, *117*(49), 31123–31133. https://doi.org/10.1073/pnas.2002437117

30. Gu, J., Wang, C., Hu, R., Li, Y., Zhang, S., Sun, Y., Wang, Q., Li, D., Fang, Y., & Liu, C. (2021). Hsp70 chaperones TDP-43 in dynamic, liquid-like phase and prevents it from amyloid aggregation. *Cell Research*, *31*(9), 1024–1027. https://doi.org/10.1038/s41422-021-00526-5

31. Hageman, J., van Waarde, M. A. W. H., Zylicz, A., Walerych, D., & Kampinga, H. H. (2011). The diverse members of the mammalian HSP70 machine show distinct chaperone-like activities. *Biochemical Journal*, *435*(1), 127–142. https://doi.org/10.1042/BJ20101247

32. Hammond, C. M., Bao, H., Hendriks, I. A., Carraro, M., García-Nieto, A., Liu, Y., Reverón-Gómez, N., Spanos, C., Chen, L., Rappsilber, J., Nielsen, M. L., Patel, D. J., Huang, H., & Groth, A. (2021). DNAJC9 integrates heat shock molecular chaperones into the histone chaperone network. *Molecular Cell*, *81*(12), 2533-2548.e9. https://doi.org/10.1016/j.molcel.2021.03.041

33. Huang, Y., Arora, K., Mun, K. S., Yang, F., Moon, C., Yarlagadda, S., Jegga, A., Weaver, T., & Naren, A. P. (2019). Targeting DNAJB9, a novel ER luminal co-chaperone, to rescue ΔF508-CFTR. *Scientific Reports*, *9*(1), 9808. https://doi.org/10.1038/s41598-019-46161-4

34. Incekara, O., & Acun, T. (2023). DNAJC9 expression in basal-like and luminal A breast cancer subtypes predicts worse survival. *Molecular Biology Reports*, *50*(9), 7275–7282. https://doi.org/10.1007/s11033-023-08654-4

35. Ito, H., Fukuda, Y., Murata, K., & Kimura, A. (1983). Transformation of intact yeast cells treated with alkali cations. *Journal of Bacteriology*, *153*(1), 163–168. https://doi.org/10.1128/jb.153.1.163-168.1983

36. Joag, H., Ghatpande, V., Desai, M., Sarkar, M., Raina, A., Shinde, M., Chitale, R., Deo, A., Bose, T., & Majumdar, A. (2020). A role of cellular translation regulation associated with toxic Huntingtin protein. *Cellular and Molecular Life Sciences*, *77*(18), 3657–3670. https://doi.org/10.1007/s00018-019-03392-y

37.Johnson, B. S., McCaffery, J. M., Lindquist, S., & Gitler, A. D. (2008a). A yeast TDP-43 proteinopathy model: Exploring the molecular determinants of TDP-43 aggregation and cellular toxicity. *Proceedings of the National Academy of Sciences*, *105*(17), 6439–6444. https://doi.org/10.1073/pnas.0802082105

38. Johnson, B. S., McCaffery, J. M., Lindquist, S., & Gitler, A. D. (2008b). A yeast TDP-43 proteinopathy model: Exploring the molecular determinants of TDP-43 aggregation and cellular toxicity. *Proceedings of the National Academy of Sciences of the United States of America*, *105*(17), 6439–6444. https://doi.org/10.1073/pnas.0802082105

39. Johnson, B. S., Snead, D., Lee, J. J., McCaffery, J. M., Shorter, J., & Gitler, A. D. (2009). TDP-43 Is Intrinsically Aggregation-prone, and Amyotrophic Lateral Sclerosis-linked Mutations Accelerate Aggregation and Increase Toxicity. *Journal of Biological Chemistry*, *284*(30), 20329–20339. https://doi.org/10.1074/jbc.M109.010264

40. Johnson, J. O., Mandrioli, J., Benatar, M., Abramzon, Y., Van Deerlin, V. M., Trojanowski, J. Q., Gibbs, J. R., Brunetti, M., Gronka, S., Wuu, J., Ding, J., McCluskey, L., Martinez-Lage, M., Falcone, D., Hernandez, D. G., Arepalli, S., Chong, S., Schymick, J. C., Rothstein, J., … Traynor, B. J. (2010). Exome Sequencing Reveals VCP Mutations as a Cause of Familial ALS. *Neuron*, *68*(5), 857–864. https://doi.org/10.1016/j.neuron.2010.11.036

41. Ju, S., Tardiff, D. F., Han, H., Divya, K., Zhong, Q., Maquat, L. E., Bosco, D. A., Hayward, L. J., Brown, R. H., Lindquist, S., Ringe, D., & Petsko, G. A. (2011). A Yeast Model of FUS/TLS-Dependent Cytotoxicity. *PLoS Biology*, *9*(4), e1001052. https://doi.org/10.1371/journal.pbio.1001052

42. Kakkar, V., Månsson, C., de Mattos, E. P., Bergink, S., van der Zwaag, M., van Waarde, M. A. W. H., Kloosterhuis, N. J., Melki, R., van Cruchten, R. T. P., Al-Karadaghi, S., Arosio, P., Dobson, C. M., Knowles, T. P. J., Bates, G. P., van Deursen, J. M., Linse, S., van de Sluis, B., Emanuelsson, C., & Kampinga, H. H. (2016). The S/T-Rich Motif in the DNAJB6 Chaperone Delays Polyglutamine Aggregation and the Onset of Disease in a Mouse Model. *Molecular Cell*, *62*(2), 272–283. https://doi.org/10.1016/j.molcel.2016.03.017

43. Kampinga, H. H., & Bergink, S. (2016). Heat shock proteins as potential targets for protective strategies in neurodegeneration. *The Lancet Neurology*, *15*(7), 748–759. https://doi.org/10.1016/S1474-4422(16)00099-5

44. Kwiatkowski, T. J., Bosco, D. A., LeClerc, A. L., Tamrazian, E., Vanderburg, C. R., Russ, C., Davis, A., Gilchrist, J., Kasarskis, E. J., Munsat, T., Valdmanis, P., Rouleau, G. A., Hosler, B. A., Cortelli, P., de Jong, P. J., Yoshinaga, Y., Haines, J. L., Pericak-Vance, M.

A., Yan, J., … Brown, R. H. (2009a). Mutations in the *FUS/TLS* Gene on Chromosome 16 Cause Familial Amyotrophic Lateral Sclerosis. *Science*, *323*(5918), 1205–1208. https://doi.org/10.1126/science.1166066

45. Kwiatkowski, T. J., Bosco, D. A., LeClerc, A. L., Tamrazian, E., Vanderburg, C. R., Russ, C., Davis, A., Gilchrist, J., Kasarskis, E. J., Munsat, T., Valdmanis, P., Rouleau, G. A., Hosler, B. A., Cortelli, P., de Jong, P. J., Yoshinaga, Y., Haines, J. L., Pericak-Vance, M. A., Yan, J., … Brown, R. H. (2009b). Mutations in the *FUS/TLS* Gene on Chromosome 16 Cause Familial Amyotrophic Lateral Sclerosis. *Science*, *323*(5918), 1205–1208. https://doi.org/10.1126/science.1166066

46. Lagier-Tourenne, C., & Cleveland, D. W. (2009). Rethinking ALS: the FUS about TDP-43. *Cell*, *136*(6), 1001–1004. https://doi.org/10.1016/j.cell.2009.03.006

47. Lagier-Tourenne, C., Polymenidou, M., & Cleveland, D. W. (2010). TDP-43 and FUS/TLS: emerging roles in RNA processing and neurodegeneration. *Human Molecular Genetics*, *19*(R1), R46–R64. https://doi.org/10.1093/hmg/ddq137

48. Lai, C. W., Otero, J. H., Hendershot, L. M., & Snapp, E. (2012). ERdj4 Protein Is a Soluble Endoplasmic Reticulum (ER) DnaJ Family Protein That Interacts with ER-associated Degradation Machinery. *Journal of Biological Chemistry*, *287*(11), 7969–7978. https://doi.org/10.1074/jbc.M111.311290

49. Li, H.-R., Chiang, W.-C., Chou, P.-C., Wang, W.-J., & Huang, J. (2018). TAR DNA-binding protein 43 (TDP-43) liquid–liquid phase separation is mediated by just a few aromatic residues. *Journal of Biological Chemistry*, *293*(16), 6090–6098. https://doi.org/10.1074/jbc.AC117.001037

50. Lindquist, S. (1981). Regulation of protein synthesis during heat shock. *Nature*, *293*(5830), 311–314. https://doi.org/10.1038/293311a0

51. Liu, D., Zuo, R., Liu, W., He, Y., Wang, Y., Yue, P., Gong, W., Cui, J., Zhu, F., Luo, Y., Qi, L., Guo, Y., Chen, L., Li, G., Liu, Z., Chen, P., & Guo, H. (2024). <scp>DNAJC24</scp> acts directly with <scp>PCNA</scp> and promotes malignant progression of <scp>LUAD</scp> by activating phosphorylation of <scp>AKT</scp>. *The FASEB Journal*, *38*(9). https://doi.org/10.1096/fj.202300667RR

52. Liu, T., Daniels, C. K., & Cao, S. (2012). Comprehensive review on the HSC70 functions, interactions with related molecules and involvement in clinical diseases and therapeutic potential. *Pharmacology & Therapeutics*, *136*(3), 354–374. https://doi.org/10.1016/j.pharmthera.2012.08.014

53. LIU, T., JIANG, W., HAN, D., & YU, L. (2012a). DNAJC25 is downregulated in hepatocellular carcinoma and is a novel tumor suppressor gene. *Oncology Letters*, *4*(6), 1274–1280. https://doi.org/10.3892/ol.2012.903

54. LIU, T., JIANG, W., HAN, D., & YU, L. (2012b). DNAJC25 is downregulated in hepatocellular carcinoma and is a novel tumor suppressor gene. *Oncology Letters*, *4*(6), 1274–1280. https://doi.org/10.3892/ol.2012.903

55. Liu, Z., Zhang, S., Gu, J., Tong, Y., Li, Y., Gui, X., Long, H., Wang, C., Zhao, C., Lu, J., He, L., Li, Y., Liu, Z., Li, D., & Liu, C. (2020). Hsp27 chaperones FUS phase separation

under the modulation of stress-induced phosphorylation. *Nature Structural & Molecular Biology*, *27*(4), 363–372. https://doi.org/10.1038/s41594-020-0399-3

56. Lorenzetti, D., Bohlega, S., & Zoghbi, H. Y. (1997). The expansion of the CAG repeat in ataxin-2 is a frequent cause of autosomal dominant spinocerebellar ataxia. *Neurology*, *49*(4), 1009–1013. https://doi.org/10.1212/WNL.49.4.1009

57. Malik, A. M., Miguez, R. A., Li, X., Ho, Y.-S., Feldman, E. L., & Barmada, S. J. (2018). Matrin 3-dependent neurotoxicity is modified by nucleic acid binding and nucleocytoplasmic localization. *ELife*, *7*. https://doi.org/10.7554/eLife.35977

58. Mandriani, B., Castellana, S., Rinaldi, C., Manzoni, M., Venuto, S., Rodriguez-Aznar, E., Galceran, J., Nieto, M. A., Borsani, G., Monti, E., Mazza, T., Merla, G., & Micale, L. (2016). Identification of p53-target genes in Danio rerio. *Scientific Reports*, *6*(1), 32474. https://doi.org/10.1038/srep32474

59. Martindale, D., Hackam, A., Wieczorek, A., Ellerby, L., Wellington, C., McCutcheon, K., Singaraja, R., Kazemi-Esfarjani, P., Devon, R., Kim, S. U., Bredesen, D. E., Tufaro, F., & Hayden, M. R. (1998). Length of huntingtin and its polyglutamine tract influences localization and frequency of intracellular aggregates. *Nature Genetics*, *18*(2), 150–154. https://doi.org/10.1038/ng0298-150

60. Mogk, A. (1999). Identification of thermolabile Escherichia coli proteins: prevention and reversion of aggregation by DnaK and ClpB. *The EMBO Journal*, *18*(24), 6934–6949. https://doi.org/10.1093/emboj/18.24.6934

61. Mogk, A., & Bukau, B. (2006). Protein quality control systems: Mechanisms and applications. *Microbial Cell Factories*, *5*(Suppl 1), S8. https://doi.org/10.1186/1475-2859-5-S1-S8

62. Molliex, A., Temirov, J., Lee, J., Coughlin, M., Kanagaraj, A. P., Kim, H. J., Mittag, T., & Taylor, J. P. (2015). Phase Separation by Low Complexity Domains Promotes Stress Granule Assembly and Drives Pathological Fibrillization. *Cell*, *163*(1), 123–133. https://doi.org/10.1016/j.cell.2015.09.015

63. Morimoto, R. I., & Santoro, M. G. (1998). Stress–inducible responses and heat shock proteins: New pharmacologic targets for cytoprotection. *Nature Biotechnology*, *16*(9), 833–838. https://doi.org/10.1038/nbt0998-833

64. Neumann, M., Sampathu, D. M., Kwong, L. K., Truax, A. C., Micsenyi, M. C., Chou, T. T., Bruce, J., Schuck, T., Grossman, M., Clark, C. M., McCluskey, L. F., Miller, B. L., Masliah, E., Mackenzie, I. R., Feldman, H., Feiden, W., Kretzschmar, H. A., Trojanowski, J. Q., & Lee, V. M.-Y. (2006a). Ubiquitinated TDP-43 in Frontotemporal Lobar Degeneration and Amyotrophic Lateral Sclerosis. *Science*, *314*(5796), 130–133. https://doi.org/10.1126/science.1134108

65. Neumann, M., Sampathu, D. M., Kwong, L. K., Truax, A. C., Micsenyi, M. C., Chou, T. T., Bruce, J., Schuck, T., Grossman, M., Clark, C. M., McCluskey, L. F., Miller, B. L., Masliah, E., Mackenzie, I. R., Feldman, H., Feiden, W., Kretzschmar, H. A., Trojanowski, J. Q., & Lee, V. M.-Y. (2006b). Ubiquitinated TDP-43 in frontotemporal

lobar degeneration and amyotrophic lateral sclerosis. *Science (New York, N.Y.)*, *314*(5796), 130–133. https://doi.org/10.1126/science.1134108

66. Park, S.-K., Hong, J. Y., Arslan, F., Kanneganti, V., Patel, B., Tietsort, A., Tank, E. M. H., Li, X., Barmada, S. J., & Liebman, S. W. (2017). Overexpression of the essential Sis1 chaperone reduces TDP-43 effects on toxicity and proteolysis. *PLoS Genetics*, *13*(5), e1006805. https://doi.org/10.1371/journal.pgen.1006805

67. R., R. K., N. S., N., S. P., A., Sinha, D., Veedin Rajan, V. B., Esthaki, V. K., & D'Silva, P. (2012). HSPIR: a manually annotated heat shock protein information resource. *Bioinformatics*, *28*(21), 2853–2855. https://doi.org/10.1093/bioinformatics/bts520

68. Richter, K., Haslbeck, M., & Buchner, J. (2010). The heat shock response: life on the verge of death. *Molecular Cell*, *40*(2), 253–266. https://doi.org/10.1016/j.molcel.2010.10.006

69. Rosen, D. R., Siddique, T., Patterson, D., Figlewicz, D. A., Sapp, P., Hentati, A., Donaldson, D., Goto, J., O'Regan, J. P., Deng, H.-X., Rahmani, Z., Krizus, A., McKenna-Yasek, D., Cayabyab, A., Gaston, S. M., Berger, R., Tanzi, R. E., Halperin, J. J., Herzfeldt, B., … Brown, R. H. (1993). Mutations in Cu/Zn superoxide dismutase gene are associated with familial amyotrophic lateral sclerosis. *Nature*, *362*(6415), 59–62. https://doi.org/10.1038/362059a0

70. Stricher, F., Macri, C., Ruff, M., & Muller, S. (2013). HSPA8/HSC70 chaperone protein. *Autophagy*, *9*(12), 1937–1954. https://doi.org/10.4161/auto.26448

71. Sun, Z., Diaz, Z., Fang, X., Hart, M. P., Chesi, A., Shorter, J., & Gitler, A. D. (2011). Molecular determinants and genetic modifiers of aggregation and toxicity for the ALS disease protein FUS/TLS. *PLoS Biology*, *9*(4), e1000614. https://doi.org/10.1371/journal.pbio.1000614

72. Thomson, D. W., & Dinger, M. E. (2016). Endogenous microRNA sponges: evidence and controversy. *Nature Reviews Genetics*, *17*(5), 272–283. https://doi.org/10.1038/nrg.2016.20

73. Ticozzi, N., Vance, C., LeClerc, A. L., Keagle, P., Glass, J. D., McKenna-Yasek, D., Sapp, P. C., Silani, V., Bosco, D. A., Shaw, C. E., Brown, R. H., & Landers, J. E. (2011). Mutational analysis reveals the *FUS* homolog *TAF15* as a candidate gene for familial amyotrophic lateral sclerosis. *American Journal of Medical Genetics Part B: Neuropsychiatric Genetics*, *156*(3), 285–290. https://doi.org/10.1002/ajmg.b.31158

74. Tomoyasu, T., Mogk, A., Langen, H., Goloubinoff, P., & Bukau, B. (2001). Genetic dissection of the roles of chaperones and proteases in protein folding and degradation in the *Escherichia coli* cytosol. *Molecular Microbiology*, *40*(2), 397–413. https://doi.org/10.1046/j.1365-2958.2001.02383.x

75. Tsai, J., & Douglas, M. G. (1996). A Conserved HPD Sequence of the J-domain Is Necessary for YDJ1 Stimulation of Hsp70 ATPase Activity at a Site Distinct from Substrate Binding. *Journal of Biological Chemistry*, *271*(16), 9347–9354. https://doi.org/10.1074/jbc.271.16.9347

76. Tummala, H., Walne, A. J., Williams, M., Bockett, N., Collopy, L., Cardoso, S., Ellison, A., Wynn, R., Leblanc, T., Fitzgibbon, J., Kelsell, D. P., van Heel, D. A., Payne, E., Plagnol, V., Dokal, I., & Vulliamy, T. (2016). DNAJC21 Mutations Link a Cancer-Prone Bone Marrow Failure Syndrome to Corruption in 60S Ribosome Subunit Maturation. *American Journal of Human Genetics*, *99*(1), 115–124. https://doi.org/10.1016/j.ajhg.2016.05.002

77. Uhrigshardt, H., Rouault, T. A., & Missirlis, F. (2013). Insertion mutants in Drosophila melanogaster Hsc20 halt larval growth and lead to reduced iron–sulfur cluster enzyme activities and impaired iron homeostasis. *JBIC Journal of Biological Inorganic Chemistry*, *18*(4), 441–449. https://doi.org/10.1007/s00775-013-0988-2

78. Vance, C., Rogelj, B., Hortobágyi, T., De Vos, K. J., Nishimura, A. L., Sreedharan, J., Hu, X., Smith, B., Ruddy, D., Wright, P., Ganesalingam, J., Williams, K. L., Tripathi, V., Al-Saraj, S., Al-Chalabi, A., Leigh, P. N., Blair, I. P., Nicholson, G., de Belleroche, J., … Shaw, C. E. (2009). Mutations in FUS, an RNA processing protein, cause familial amyotrophic lateral sclerosis type 6. *Science (New York, N.Y.)*, *323*(5918), 1208–1211. https://doi.org/10.1126/science.1165942

79. Vance, C., Rogelj, B., Hortobágyi, T., De Vos, K. J., Nishimura, A. L., Sreedharan, J., Hu, X., Smith, B., Ruddy, D., Wright, P., Ganesalingam, J., Williams, K. L., Tripathi, V., Al-Saraj, S., Al-Chalabi, A., Leigh, P. N., Blair, I. P., Nicholson, G., de Belleroche, J., … Shaw, C. E. (2009). Mutations in FUS, an RNA Processing Protein, Cause Familial Amyotrophic Lateral Sclerosis Type 6. *Science*, *323*(5918), 1208–1211. https://doi.org/10.1126/science.1165942

80. Veenma, D., Cordeiro, D., Sondheimer, N., & Mercimek-Andrews, S. (2018). DNAJC12-associated developmental delay, movement disorder, and mild hyperphenylalaninemia identified by whole-exome sequencing re-analysis. *European Journal of Human Genetics*, *26*(12), 1867–1870. https://doi.org/10.1038/s41431-018-0237-9

81. Warrick, J. M., Chan, H. Y. E., Gray-Board, G. L., Chai, Y., Paulson, H. L., & Bonini, N. M. (1999). Suppression of polyglutamine-mediated neurodegeneration in Drosophila by the molecular chaperone HSP70. *Nature Genetics*, *23*(4), 425–428. https://doi.org/10.1038/70532

82. Watanabe, M., Dykes-Hoberg, M., Cizewski Culotta, V., Price, D. L., Wong, P. C., & Rothstein, J. D. (2001). Histological Evidence of Protein Aggregation in Mutant SOD1 Transgenic Mice and in Amyotrophic Lateral Sclerosis Neural Tissues. *Neurobiology of Disease*, *8*(6), 933–941. https://doi.org/10.1006/nbdi.2001.0443

83. Wu, E., He, W., Wu, C., Chen, Z., Zhou, S., Wu, X., Hu, Z., Jia, K., Pan, J., Wang, L., Qin, J., Liu, D., Lu, J., Wang, H., Li, J., Wang, S., & Sun, L. (2023). HSPA8 acts as an amyloidase to suppress necroptosis by inhibiting and reversing functional amyloid formation. *Cell Research*, *33*(11), 851–866. https://doi.org/10.1038/s41422-023-00859-3

84. Yabe, I., Tanino, M., Yaguchi, H., Takiyama, A., Cai, H., Kanno, H., Takahashi, I., Hayashi, Y. K., Watanabe, M., Takahashi, H., Hatakeyama, S., Tanaka, S., & Sasaki, H. (2014). Pathology of frontotemporal dementia with limb girdle muscular dystrophy

1038 caused by a DNAJB6 mutation. *Clinical Neurology and Neurosurgery*, *127*, 10–12.
1039 https://doi.org/10.1016/j.clineuro.2014.09.013

1040 85. Zhang, Z., Jing, J., Ye, Y., Chen, Z., Jing, Y., Li, S., Hong, W., Ruan, H., Liu, Y., Hu, Q.,
1041 Wang, J., Li, W., Lin, C., Diao, L., Zhou, Y., & Han, L. (2020). Characterization of the
1042 dual functional effects of heat shock proteins (HSPs) in cancer hallmarks to aid
1043 development of HSP inhibitors. *Genome Medicine*, *12*(1), 101.
1044 https://doi.org/10.1186/s13073-020-00795-6

1045 1.

1046 **12.0 Supplementary figures**

1047 **Supplementary Fig S1. TDP-43 and FUS plasmid.**

1048 ALS plasmid TDP-43 and FUS sequence map.

1049

1050 **Supplementary Fig S2. ALS mutants TDP-43 and FUS and their effect on toxicity in**

1051 **yeast cells.**

1052 **S2a.** Spot dilution of plasmids TDP-43 and FUS with control after transformation in yeast.

1053 **S2b.** 48hrs growth curve of TDP-43 and FUS, obtaining O.D. after 30 min at 600 nm (n=3,

1054 P<0.05, paired t-test).

1055 **S2b.** Confocal Microscopy of GFP-tagged plasmids TDP-43 and FUS with control.

1056

1057 **Supplementary Fig S3. DnaJ domain chaperones overexpression library construction.**

1058 DnaJ domain chaperones overexpression library was created from flies, which are

1059 homologous to the DnaJ domain proteins of humans, by Gateway cloning.

1060

1061 **Supplementary Fig S4. Effect of mutant TDP-43 and DnaJ chaperones on growth**

1062 **S4a.** Enhancers and suppressors of TDP-43 are characterized based on the spot dilution assay
1063 on the control plate SD-Trp-Ura.

1064 **S4c.** Weak enhancer and suppressor classification based on spot dilution assay of TDP-43
1065 chaperones on control SD-Trp-Ura.

1066

1067 **Supplementary Fig S5. Effect of mutant FUS and DnaJ chaperones on growth**

1068 **S5a.**Enhancers and suppressors of FUS are characterized based on the spot dilution assay on
1069 the control plate SD-Trp-Ura.

1070 **S4c.**Weak enhancer and suppressor classification of FUS chaperones on control SD-Trp-Ura.

1071

1072 **Supplementary Fig S6. Phylogenetic tree for Hsp40 chaperones**

1073 A phylogenetic tree was created using the Mega12 tool by using multiple sequence alignment
1074 of chaperones, showing region of protein conserved across species.

1075

1076 **Supplementary Table 1 Plasmid genotype and yeast strains.**

1077 In supplementary Table1 genotype of yeast strain, TDP-43 and FUS plasmid as well as
1078 chaperone genotype, were mentioned**.**

1079

1080 **Supplementary Table 2 DnaJ domain chaperones and their related functions**

1081 In this table, mentioned about homologue/orthologue of the *Drosophila* DnaJ domain
1082 chaperone as well as their predicted functions.

Fig1 a

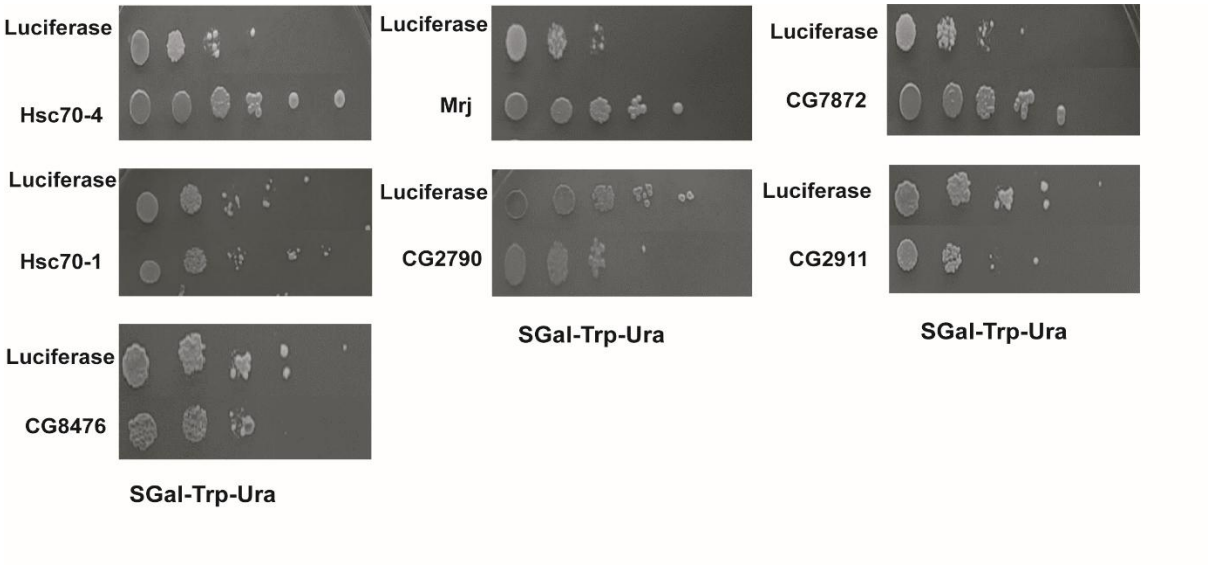
Luciferase
Hsc70-4
Luciferase
Mrj
Luciferase
CG7872
Luciferase
Hsc70-1
Luciferase
CG2790
Luciferase
CG2911
SGal-Trp-Ura
SGal-Trp-Ura
Luciferase
CG8476
SGal-Trp-Ura

1b

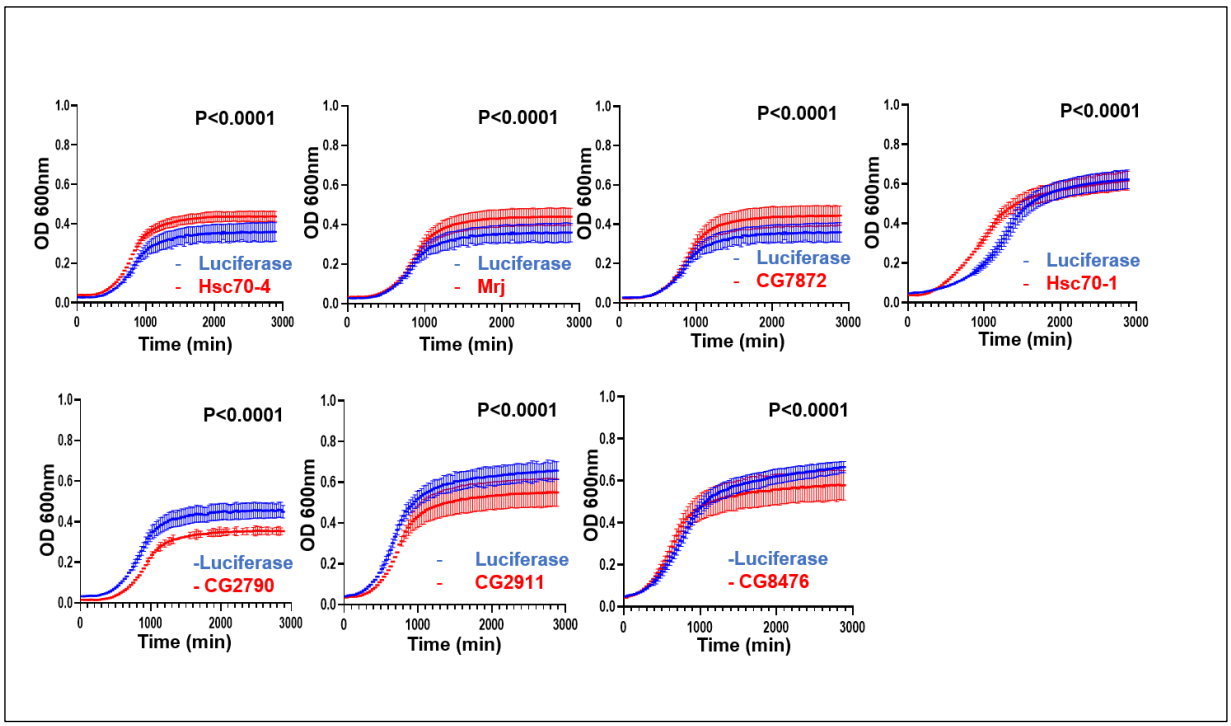
P<0.0001
OD 600nm
Time (min)
- Luciferase
- Hsc70-4
- Luciferase
- Mrj
- Luciferase
- CG7872
- Luciferase
- Hsc70-1
-Luciferase
- CG2790
- Luciferase
- CG2911
-Luciferase
- CG8476

1c

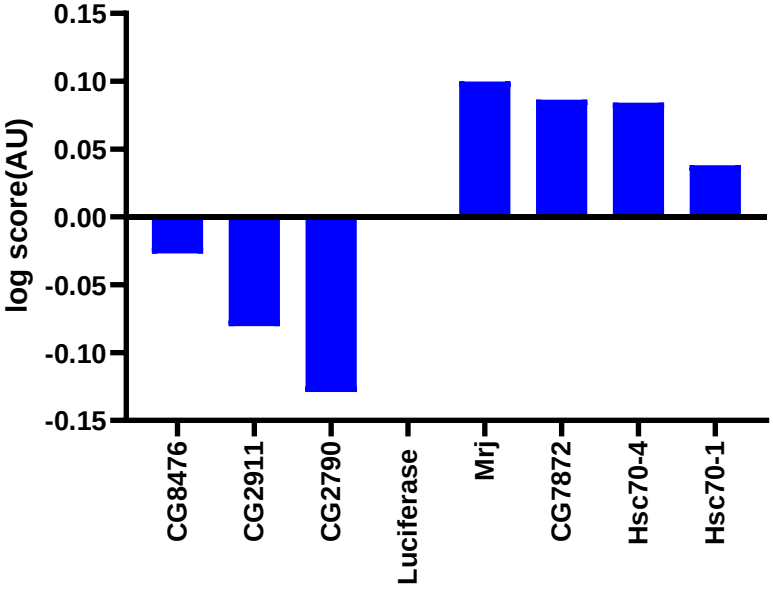
0.15
0.10
0.05
0.00
-0.05
-0.10
-0.15
log score(AU)
CG8476
CG2911
CG2790
Luciferase
Mrj
CG7872
Hsc70-4
Hsc70-1

1d

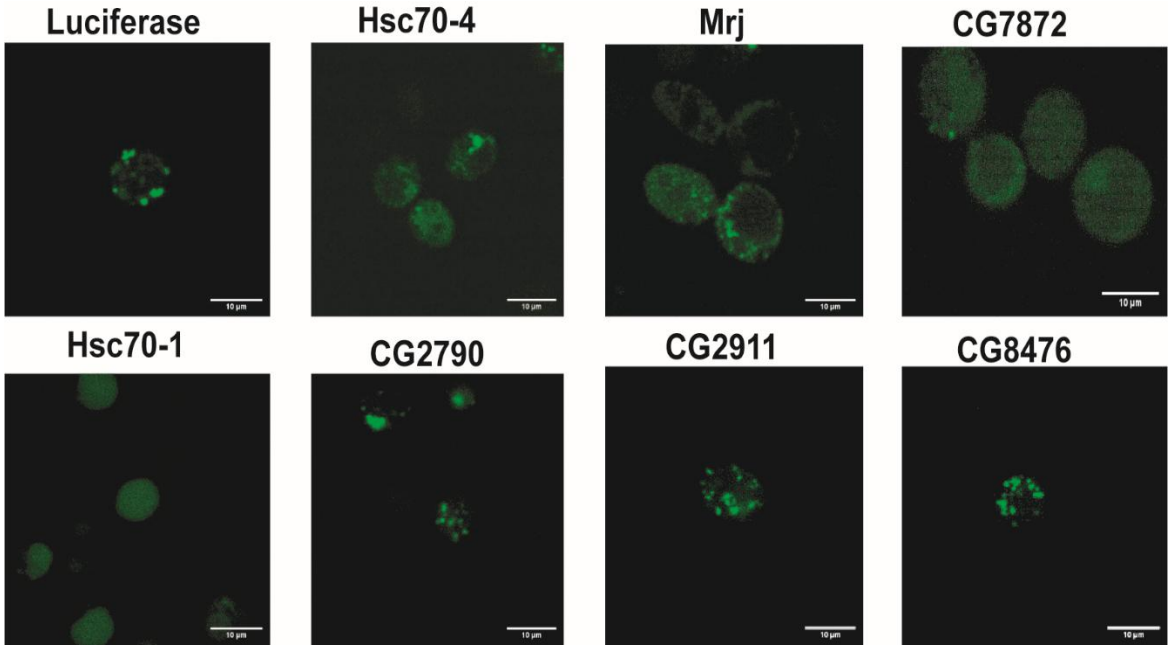
Luciferase
Hsc70-4
Mrj
CG7872
Hsc70-1
CG2790
CG2911
CG8476

1e

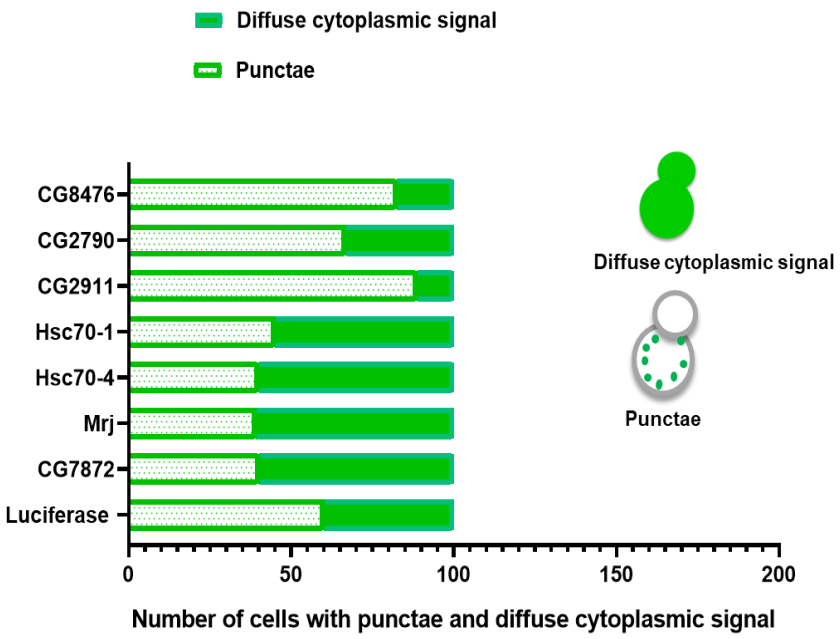

Table 2

	Puncta	Diffuse cytoplasmic signal
Luciferase	60.10	39.90
CG7872	40.22	59.70
Mrj	39.20	60.80
Hsc70-4	40.00	60.00
Hsc70-1	45.00	55.00
CG2911	88.80	11.11
CG2790	66.80	33.20
CG8476	82.50	17.50

Fig2 a

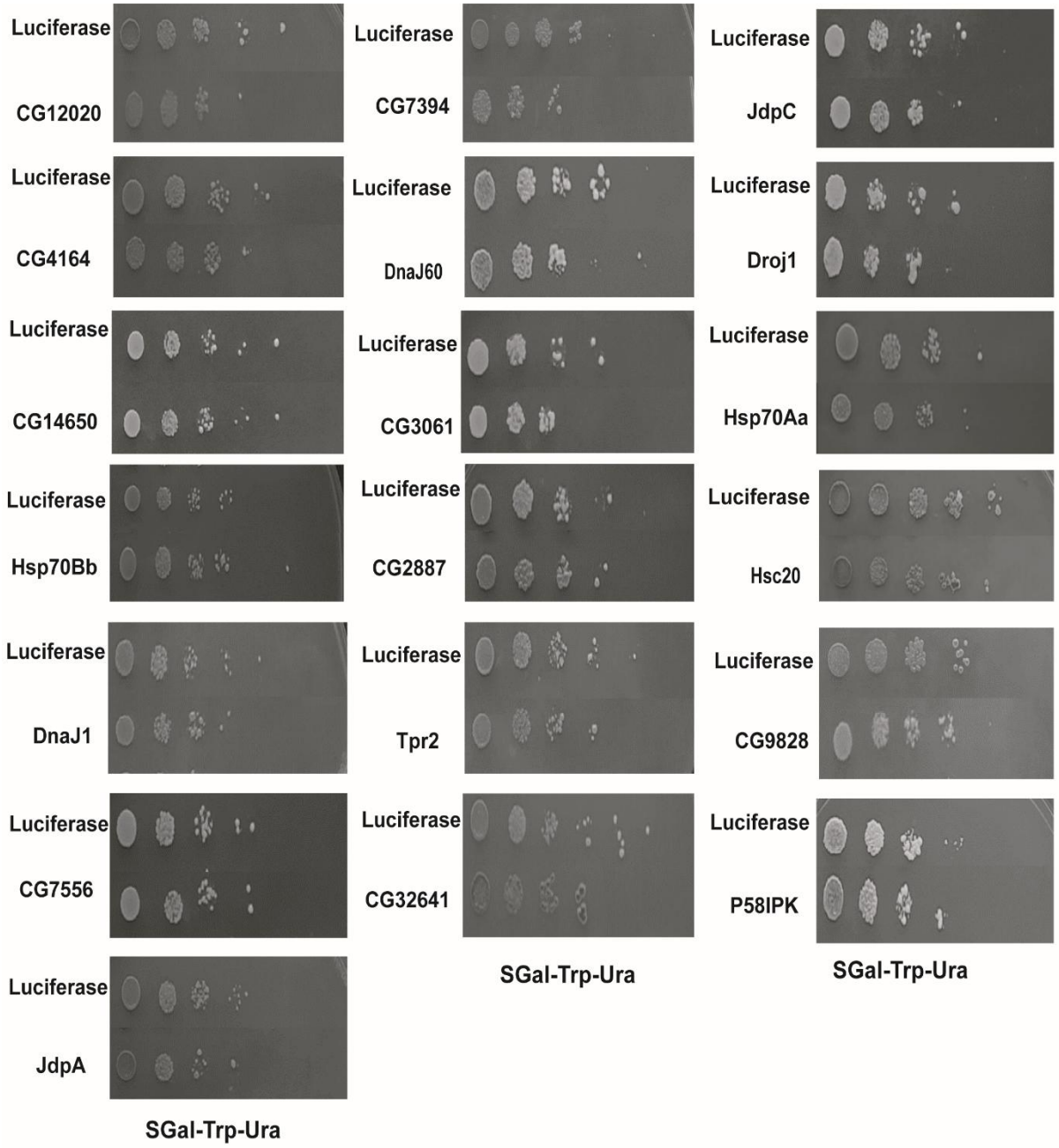
Luciferase
CG12020
Luciferase
CG4164
Luciferase
CG14650
Luciferase
Hsp70Bb
Luciferase
DnaJ1
Luciferase
CG7556
Luciferase
JdpA
SGal-Trp-Ura
Luciferase
CG7394
Luciferase
DnaJ60
Luciferase
CG3061
Luciferase
CG2887
Luciferase
Tpr2
Luciferase
CG32641
SGal-Trp-Ura
Luciferase
JdpC
Luciferase
Droj1
Luciferase
Hsp70Aa
Luciferase
Hsc20
Luciferase
CG9828
Luciferase
P58IPK
SGal-Trp-Ura

2b

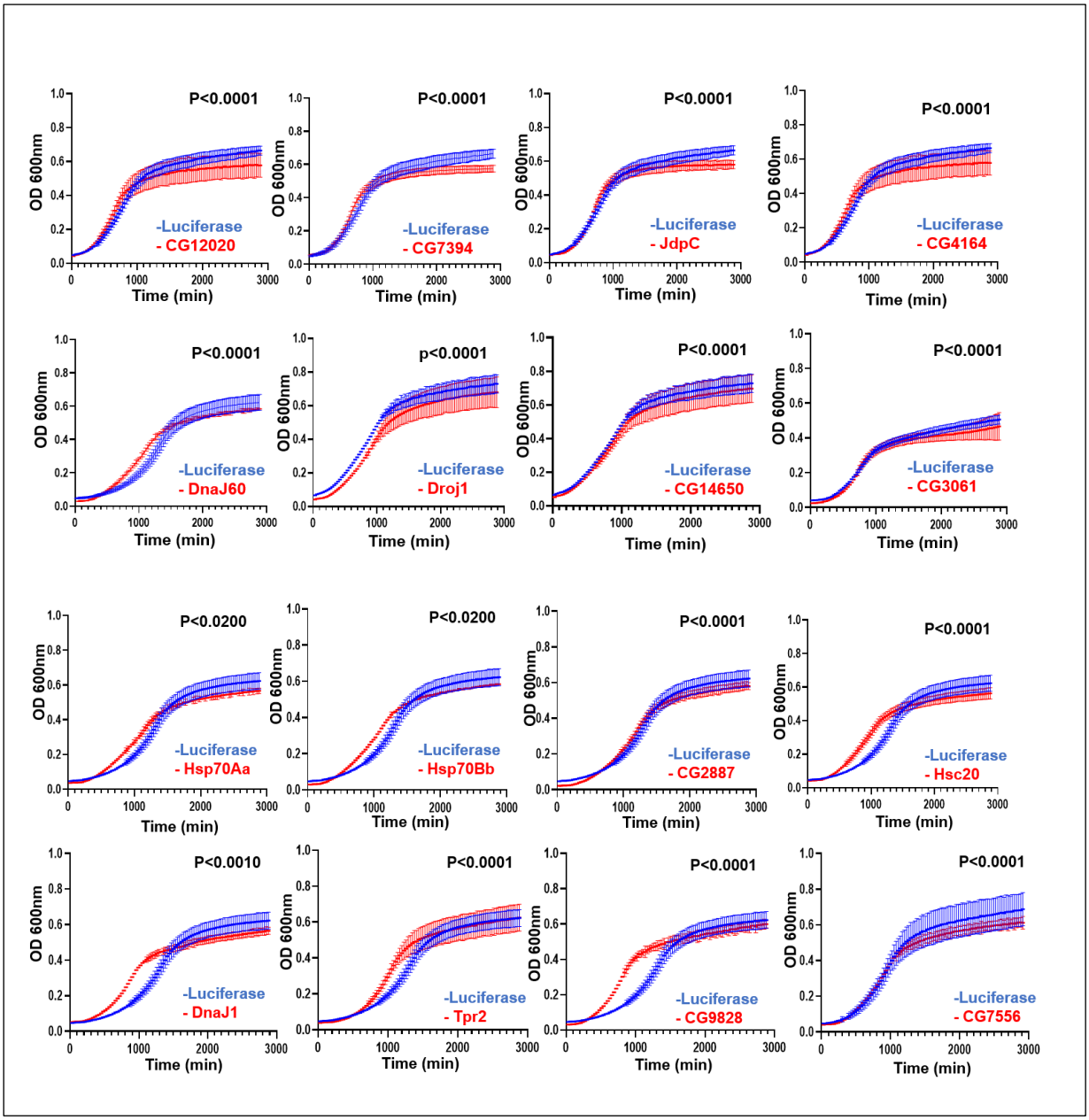
P<0.0001
-Luciferase
- CG12020
P<0.0001
-Luciferase
- CG7394
P<0.0001
-Luciferase
- JdpC
P<0.0001
-Luciferase
- CG4164
P<0.0001
-Luciferase
- DnaJ60
p<0.0001
-Luciferase
- Droj1
P<0.0001
-Luciferase
- CG14650
P<0.0001
-Luciferase
- CG3061
P<0.0200
-Luciferase
- Hsp70Aa
P<0.0200
-Luciferase
- Hsp70Bb
P<0.0001
-Luciferase
- CG2887
P<0.0001
-Luciferase
- Hsc20
P<0.0010
-Luciferase
- DnaJ1
P<0.0001
-Luciferase
- Tpr2
P<0.0001
-Luciferase
- CG9828
P<0.0001
-Luciferase
- CG7556
OD 600nm
Time (min)

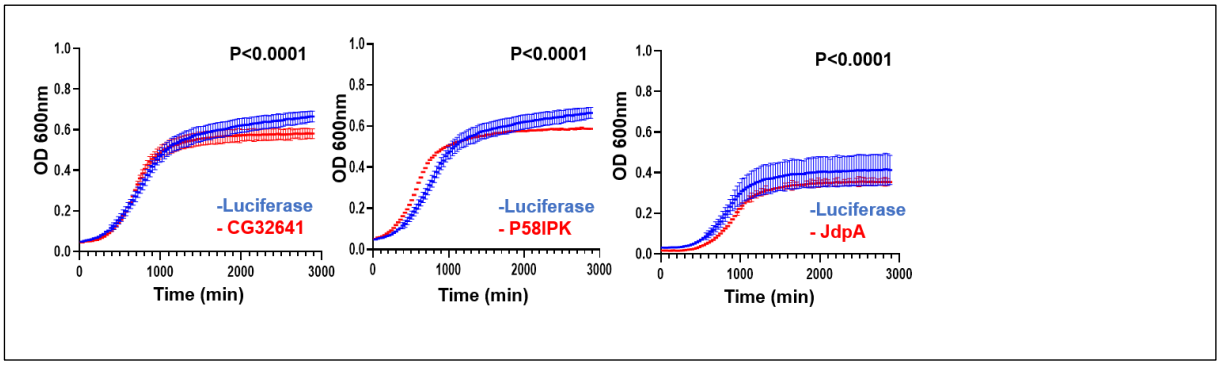
P<0.0001
-Luciferase
- CG32641
P<0.0001
-Luciferase
- P58IPK
P<0.0001
-Luciferase
- JdpA
OD 600nm
Time (min)

2c

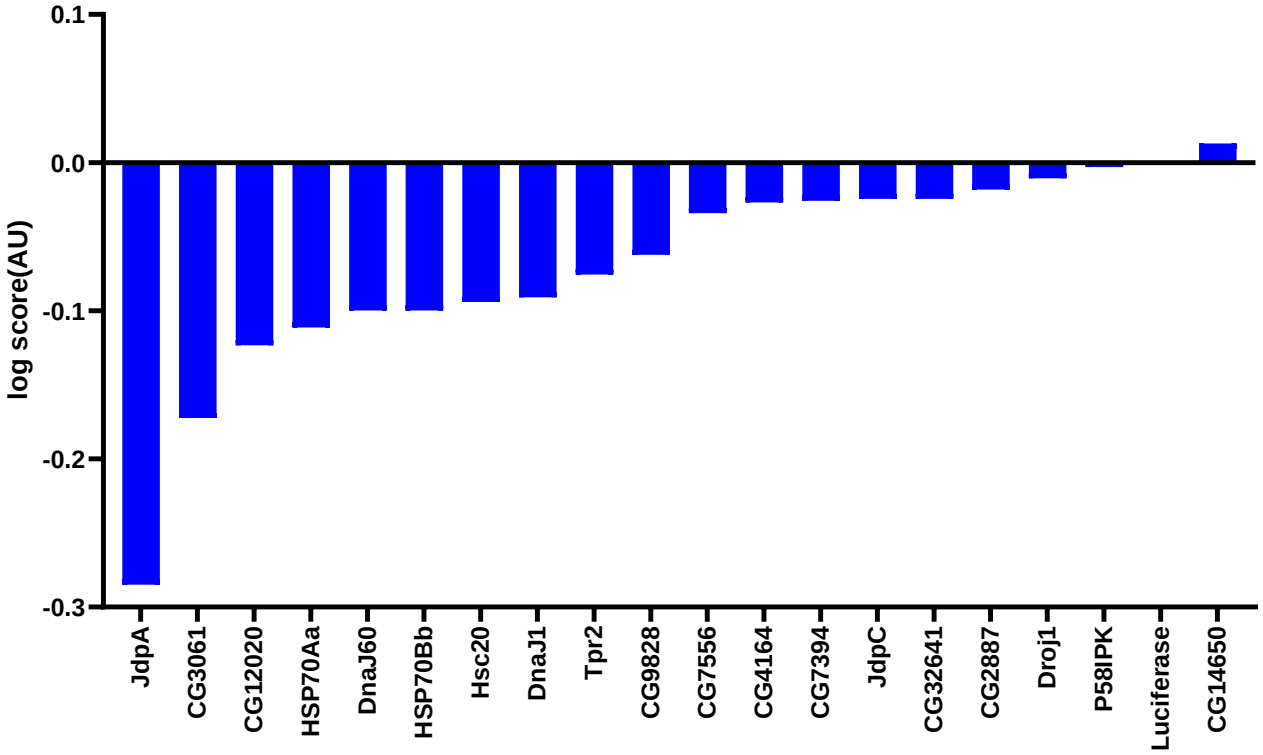
0.1
0.0
-0.1
-0.2
-0.3
log score(AU)
JdpA
CG3061
CG12020
HSP70Aa
DnaJ60
HSP70Bb
Hsc20
DnaJ1
Tpr2
CG9828
CG7556
CG4164
CG7394
JdpC
CG32641
CG2887
Droj1
P58IPK
Luciferase
CG14650

2d

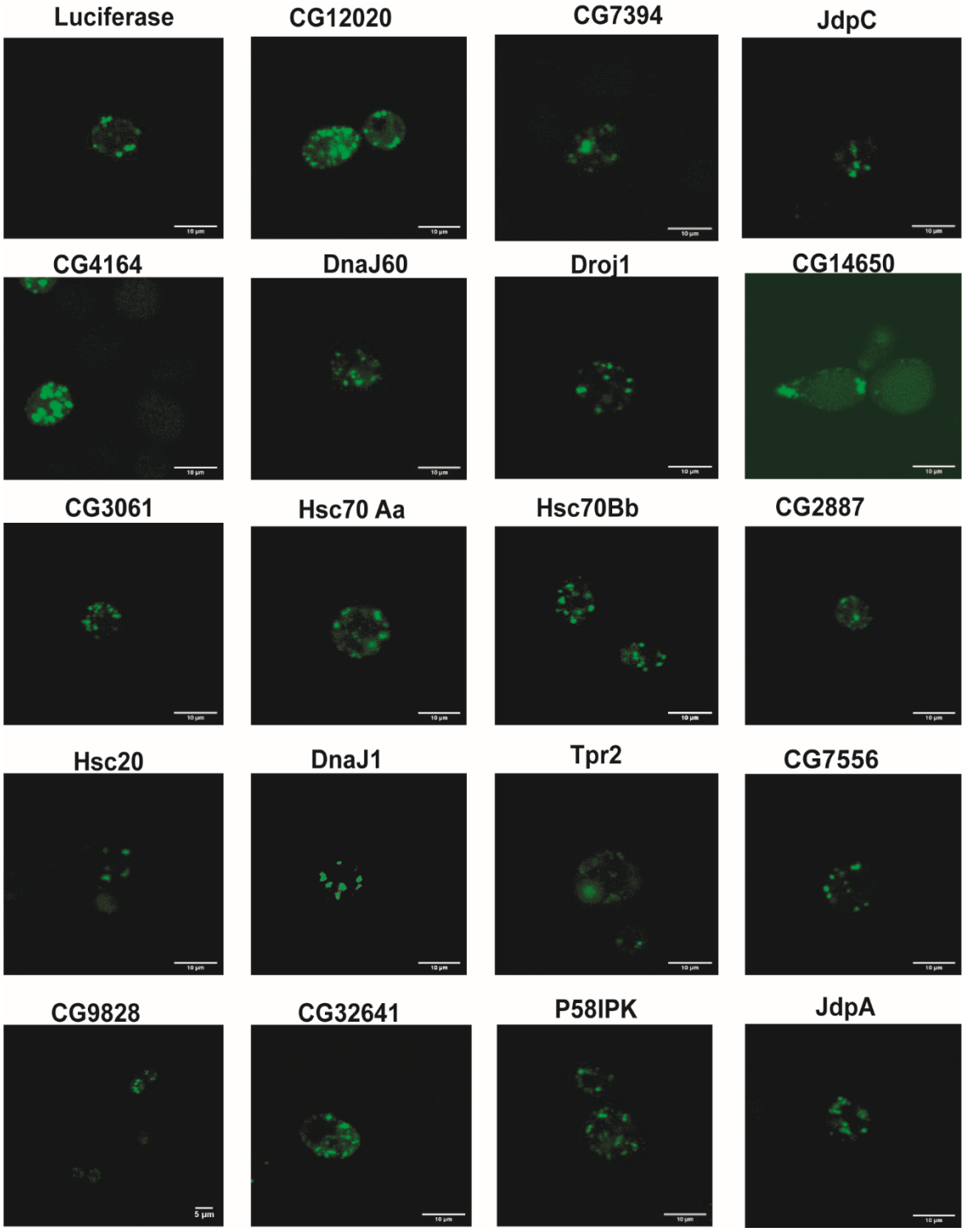
Luciferase
CG12020
CG7394
JdpC
CG4164
DnaJ60
Droj1
CG14650
CG3061
Hsc70 Aa
Hsc70Bb
CG2887
Hsc20
DnaJ1
Tpr2
CG7556
CG9828
CG32641
P58IPK
JdpA

2e

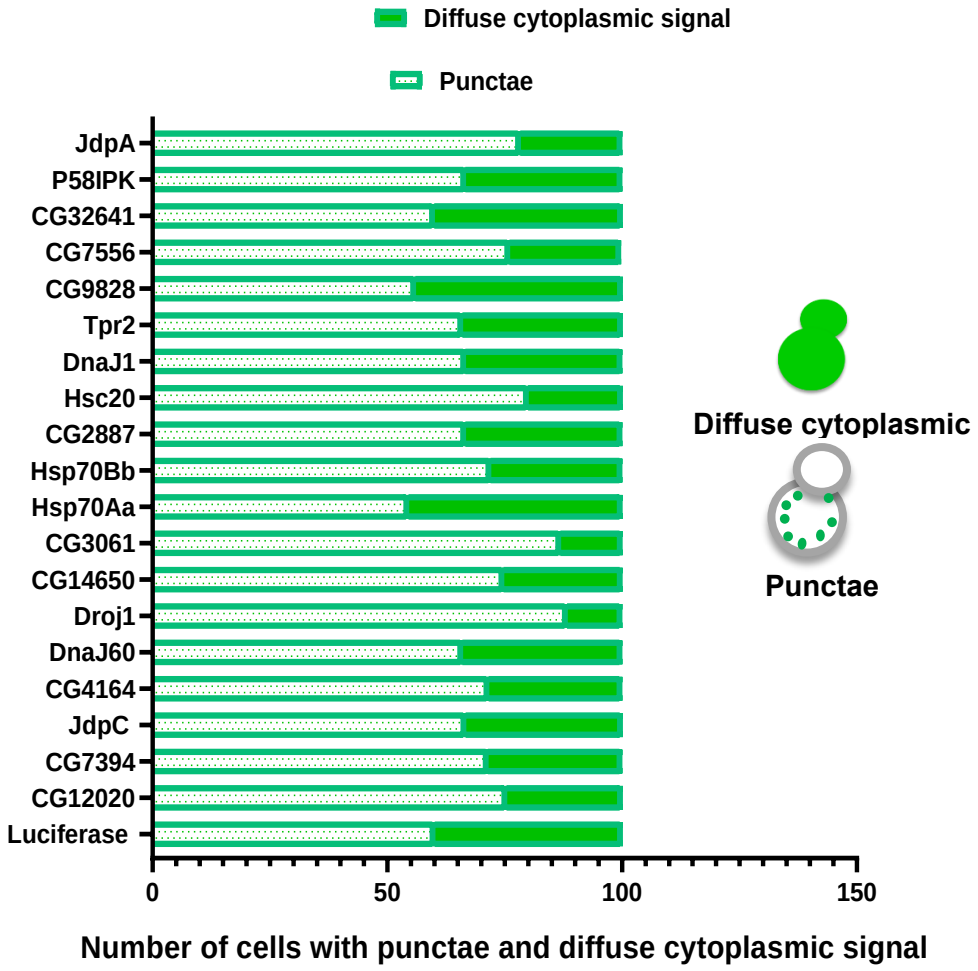

Table 3

	Puncta	Diffuse cytoplasmic signal
Luciferase	60.10	39.90
CG12020	75.38	24.62
CG7394	71.40	28.50
JdpC	66.66	33.34
CG4164	71.60	28.30
DnaJ60	66.00	33.90
Droj1	88.30	11.60
CG14650	74.79	25.20
CG3061	86.88	13.11
Hsp70Aa	54.54	45.45
Hsp70Bb	72.00	27.90
CG2887	66.60	33.30
Hsc20	80.00	20.00
DnaJ1	66.60	33.30
Tpr2	66.00	34.00
CG9828	56.00	44.00
CG7556	76.00	23.68
CG32641	60.00	40.00
P58IPK	66.60	33.30
JdpA	78.30	21.60

Fig 1f

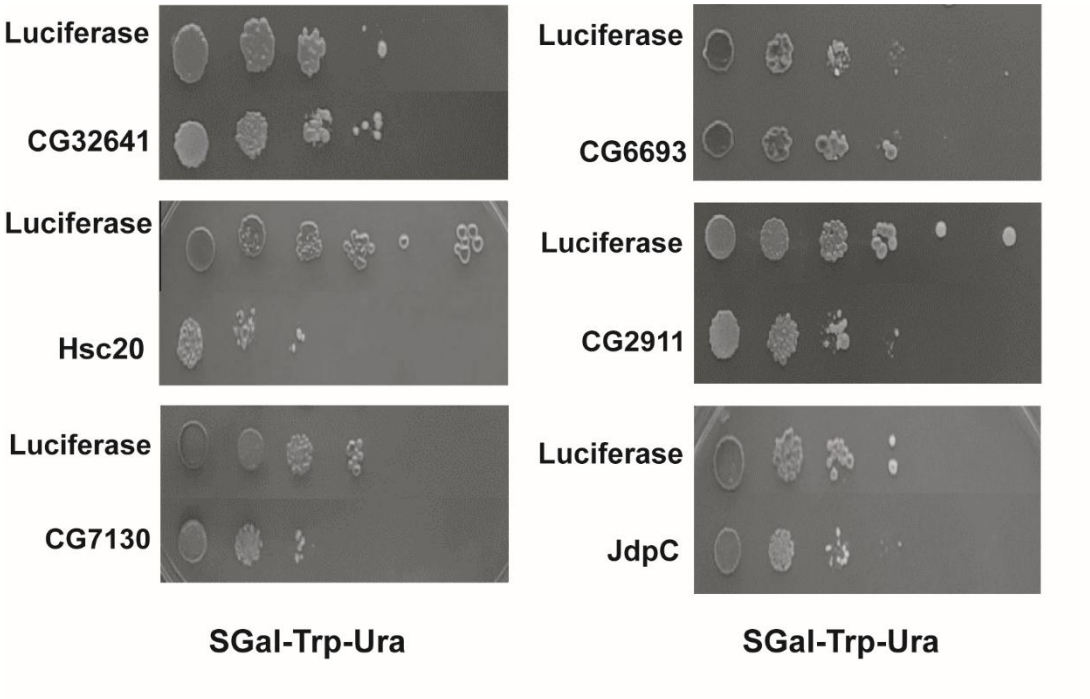
Luciferase
CG32641
Luciferase
CG6693
Luciferase
Hsc20
Luciferase
CG2911
Luciferase
CG7130
Luciferase
JdpC
SGal-Trp-Ura
SGal-Trp-Ura

1g

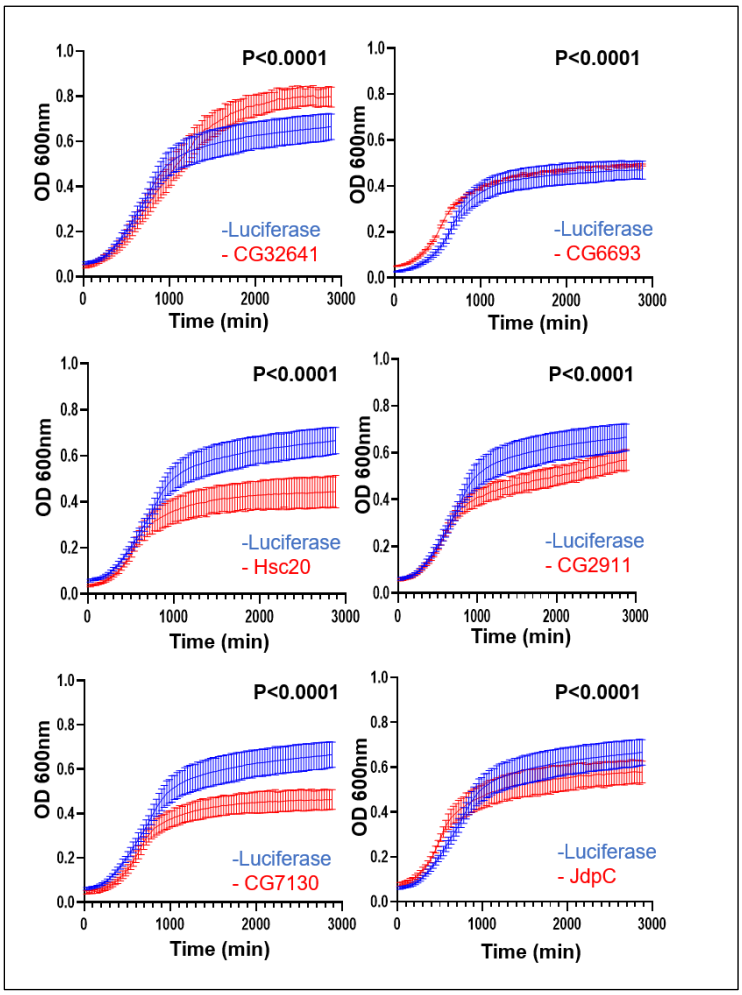
P<0.0001
OD 600nm
Time (min)
-Luciferase
- CG32641
P<0.0001
OD 600nm
Time (min)
-Luciferase
- CG6693
P<0.0001
OD 600nm
Time (min)
-Luciferase
- Hsc20
P<0.0001
OD 600nm
Time (min)
-Luciferase
- CG2911
P<0.0001
OD 600nm
Time (min)
-Luciferase
- CG7130
P<0.0001
OD 600nm
Time (min)
-Luciferase
- JdpC

1h

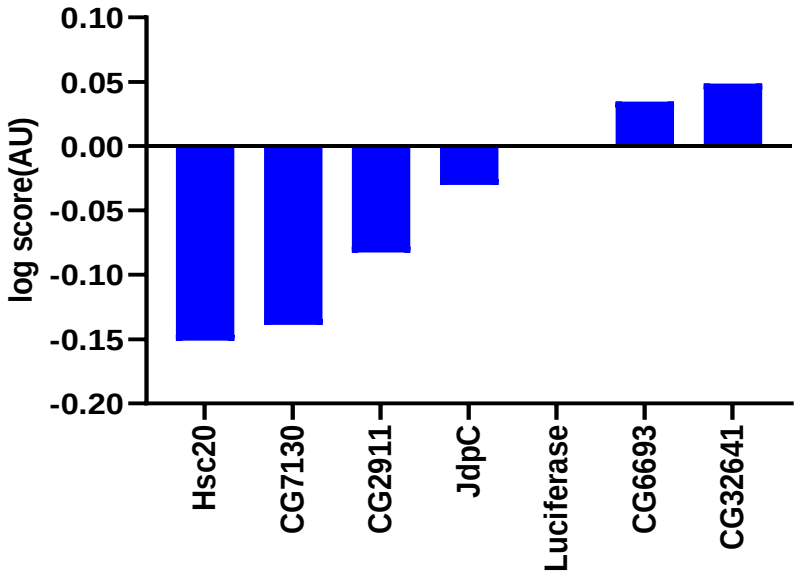
0.10
0.05
0.00
-0.05
-0.10
-0.15
-0.20
log score(AU)
Hsc20
CG7130
CG2911
JdpC
Luciferase
CG6693
CG32641

1i

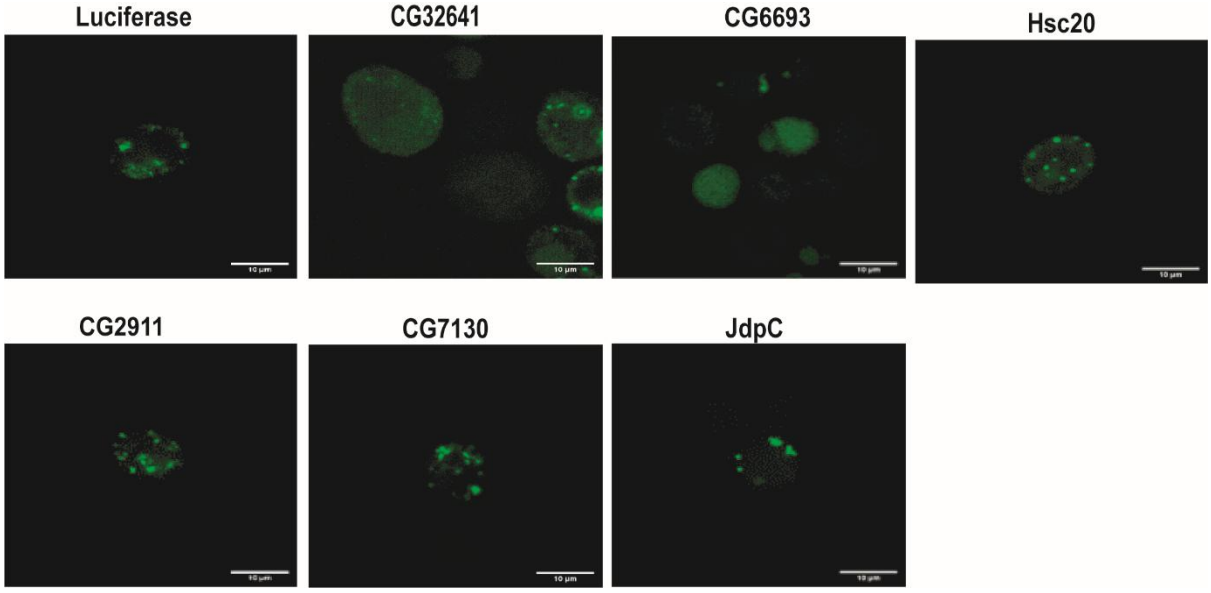
Luciferase
CG32641
CG6693
Hsc20
CG2911
CG7130
JdpC

1j

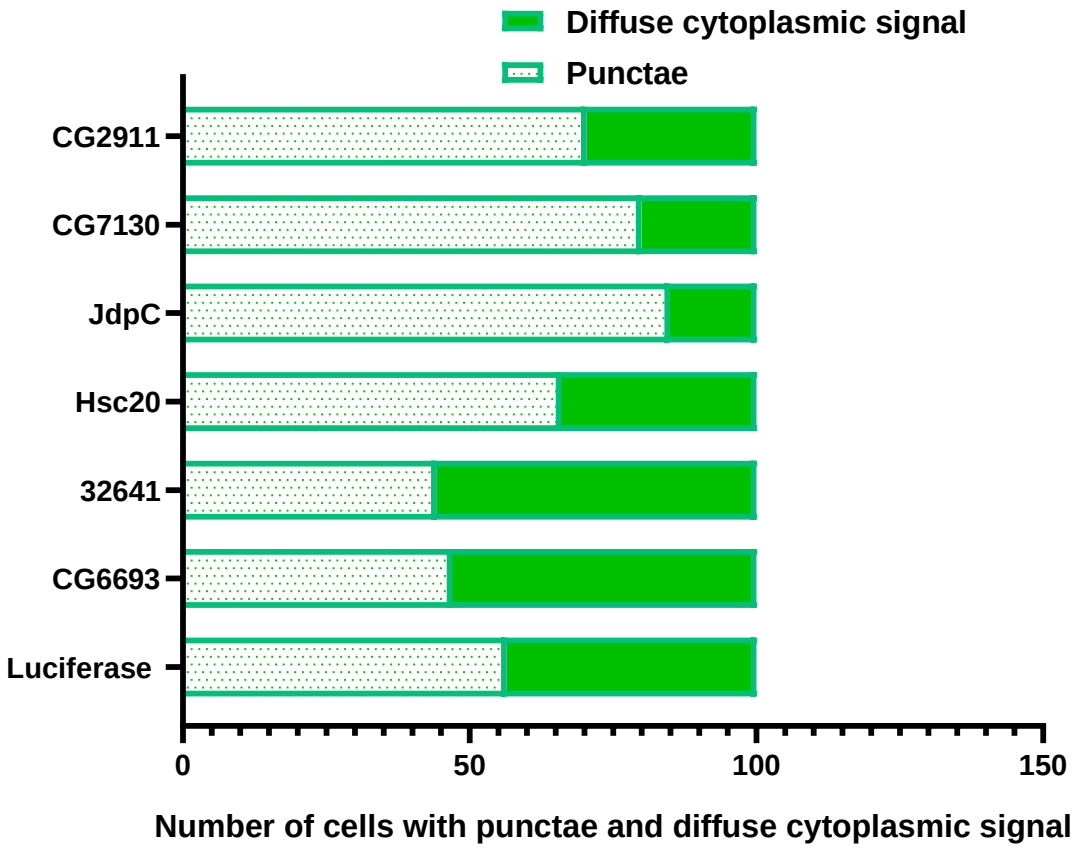

Table 4

	Punctae	Diffuse cytoplasmic signal
Luciferase	56.52	43.48
CG6693	47.00	53.00
32641	44.29	55.71
Hsc20	66.00	34.00
JdpC	85.00	15.00
CG7130	80.00	20.00
CG2911	70.45	29.55

Fig 2f

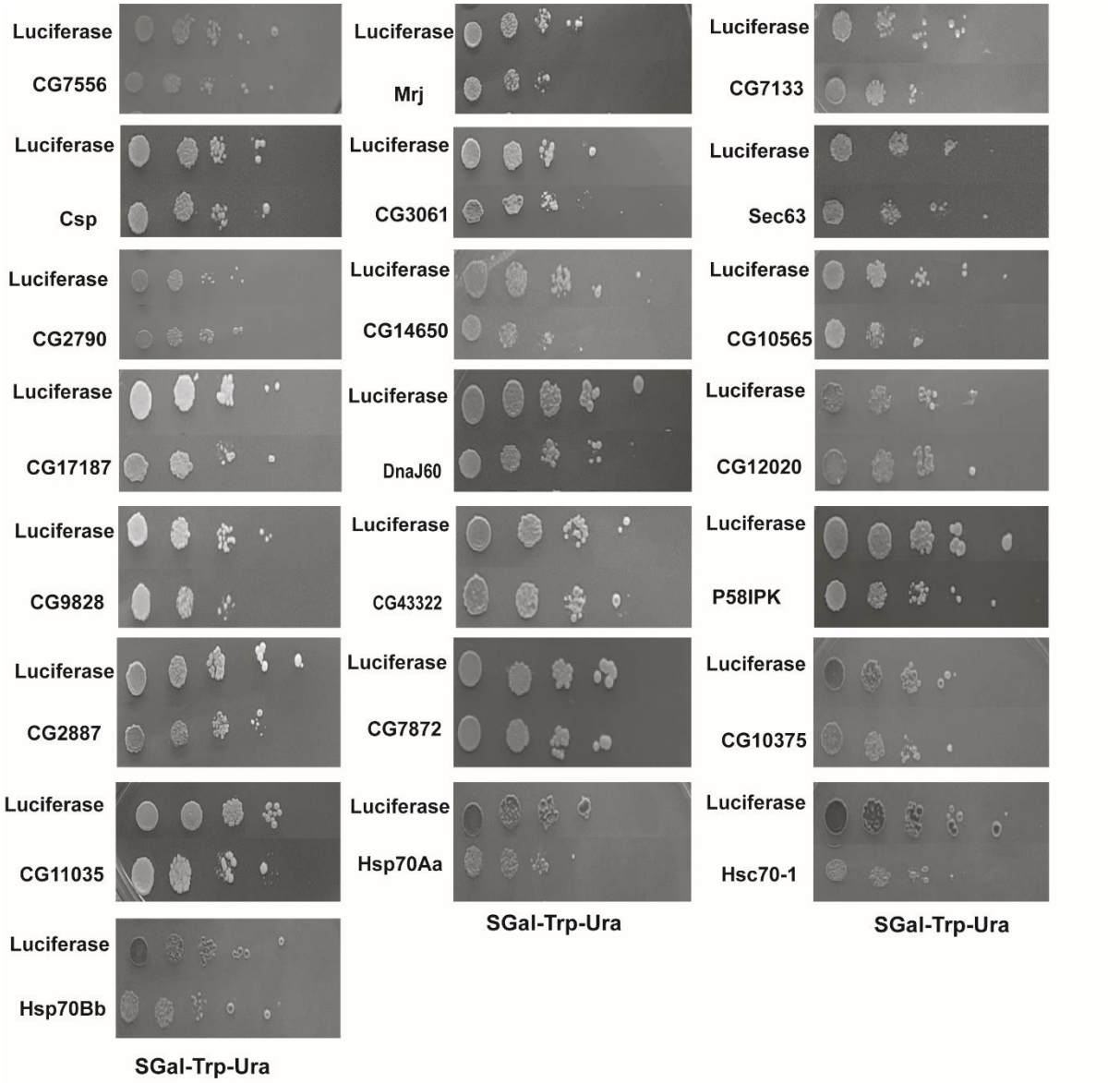
Luciferase
CG7556
Luciferase
Csp
Luciferase
CG2790
Luciferase
CG17187
Luciferase
CG9828
Luciferase
CG2887
Luciferase
CG11035
Luciferase
Hsp70Bb
SGal-Trp-Ura
Luciferase
Mrj
Luciferase
CG3061
Luciferase
CG14650
Luciferase
DnaJ60
Luciferase
CG43322
Luciferase
CG7872
Luciferase
Hsp70Aa
SGal-Trp-Ura
Luciferase
CG7133
Luciferase
Sec63
Luciferase
CG10565
Luciferase
CG12020
Luciferase
P58IPK
Luciferase
CG10375
Luciferase
Hsc70-1
SGal-Trp-Ura

2g

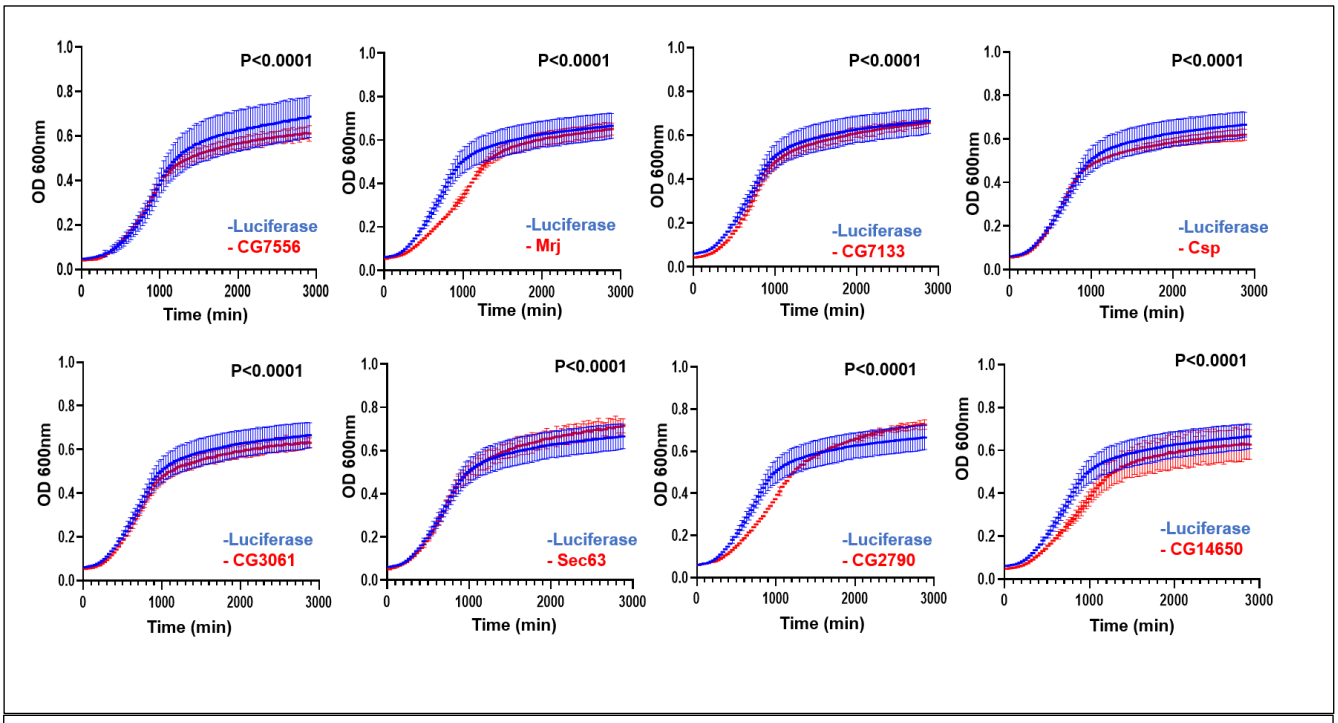
P<0.0001
-Luciferase
- CG7556
P<0.0001
-Luciferase
- Mrj
P<0.0001
-Luciferase
- CG7133
P<0.0001
-Luciferase
- Csp
P<0.0001
-Luciferase
- CG3061
P<0.0001
-Luciferase
- Sec63
P<0.0001
-Luciferase
- CG2790
P<0.0001
-Luciferase
- CG14650
OD 600nm
Time (min)

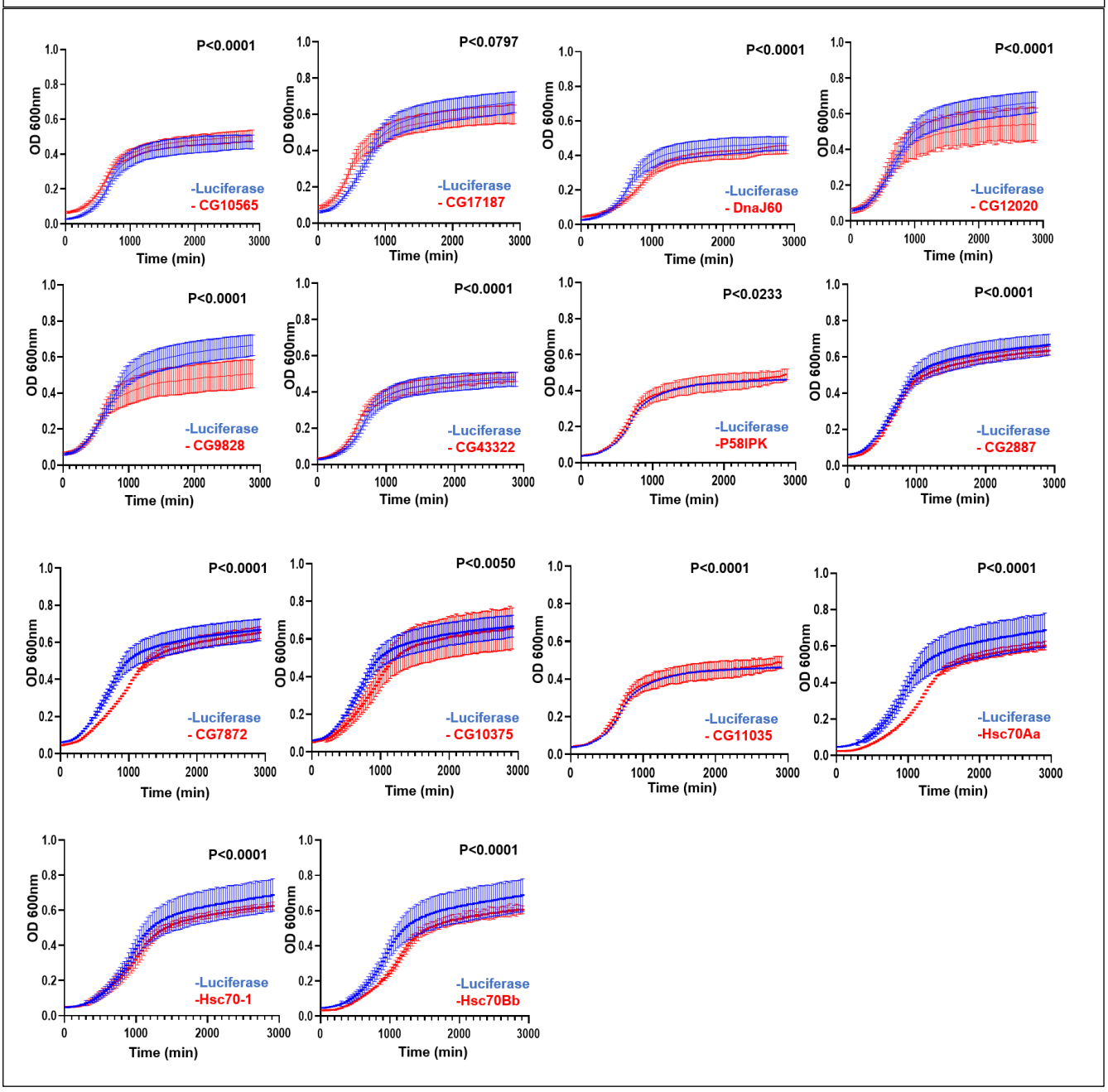
P<0.0001
-Luciferase
- CG10565
P<0.0797
-Luciferase
- CG17187
P<0.0001
-Luciferase
- DnaJ60
P<0.0001
-Luciferase
- CG12020
P<0.0001
-Luciferase
- CG9828
P<0.0001
-Luciferase
- CG43322
P<0.0233
-Luciferase
-P58IPK
P<0.0001
-Luciferase
- CG2887
P<0.0001
-Luciferase
- CG7872
P<0.0050
-Luciferase
- CG10375
P<0.0001
-Luciferase
- CG11035
P<0.0001
-Luciferase
-Hsc70Aa
P<0.0001
-Luciferase
-Hsc70-1
P<0.0001
-Luciferase
-Hsc70Bb
OD 600nm
Time (min)

2h

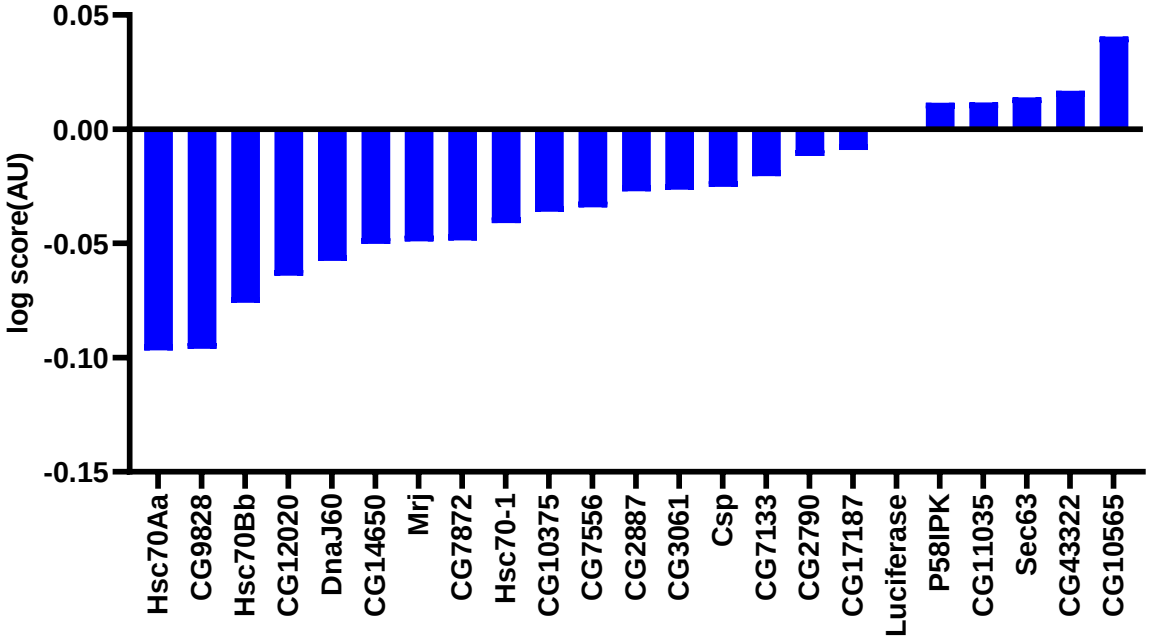
0.05
0.00
-0.05
-0.10
-0.15
log score(AU)
Hsc70Aa
CG9828
Hsc70Bb
CG12020
DnaJ60
CG14650
Mrj
CG7872
Hsc70-1
CG10375
CG7556
CG2887
CG3061
Csp
CG7133
CG2790
CG17187
Luciferase
P58IPK
CG11035
Sec63
CG43322
CG10565

2i

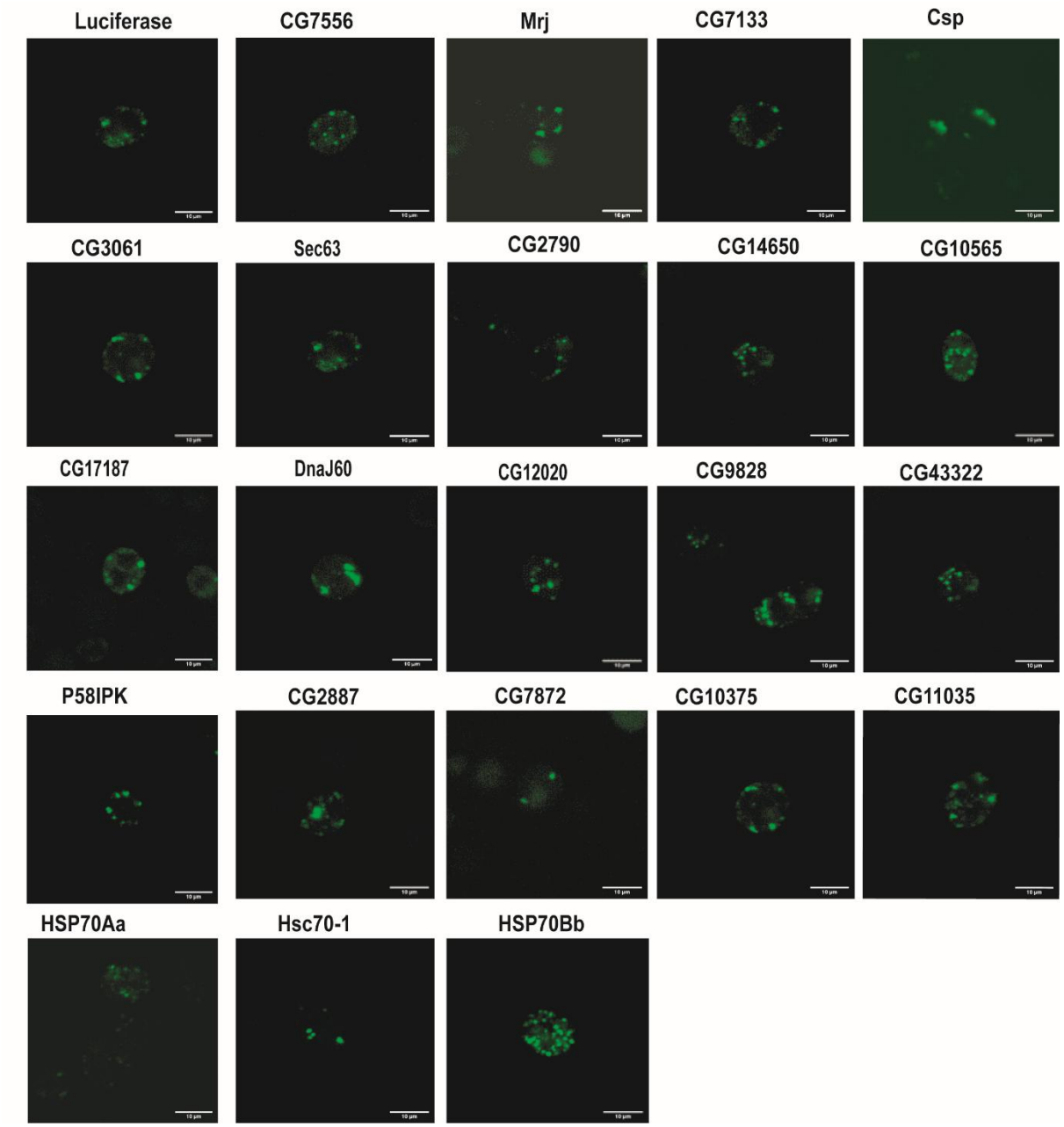
Luciferase
CG7556
Mrj
CG7133
Csp
CG3061
Sec63
CG2790
CG14650
CG10565
CG17187
DnaJ60
CG12020
CG9828
CG43322
P58IPK
CG2887
CG7872
CG10375
CG11035
HSP70Aa
Hsc70-1
HSP70Bb

2j

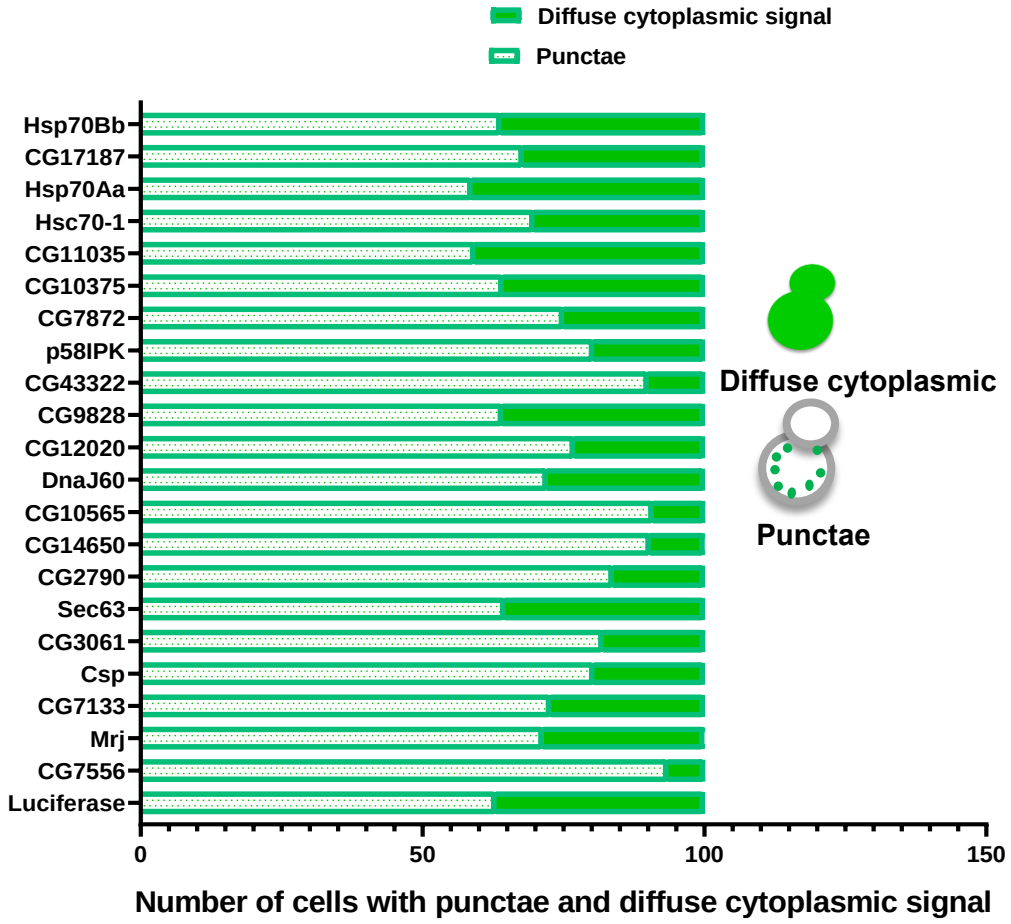

Table 5

	Punctae	Diffuse cytoplasmic signal
Luciferase	63.04	36.95
CG7556	93.54	6.46
Mrj	71.40	28.50
CG7133	72.72	27.27
Csp	80.39	19.60
CG3061	82.00	18.00
Sec63	64.61	35.38
CG2790	83.80	16.19
CG14650	90.40	9.52
CG10565	90.90	9.10
DnaJ60	72.09	27.90
CG12020	76.92	23.07
CG9828	64.17	35.82
CG43322	90.00	10.00
p58IPK	80.35	19.64
CG7872	75.00	25.00
CG10375	64.28	35.71
CG11035	59.25	40.74
Hsc70-1	69.76	30.23
Hsp70Aa	58.76	41.23
CG17187	67.85	32.14
Hsp70Bb	63.88	36.12